MAX IV Beamline Review Report

FlexPES

September 2022

Beamline Review Report

The FlexPES beamline team

September 2022

Contents

1 General introduction

FlexPES is a soft x-ray (40 – 1500 eV) beamline on the 1.5 GeV storage ring at the MAX IV Laboratory, with the focus on photoelectron spectroscopy (PES), x-ray absorption spectroscopy (XAS) and electron-ion coincidence techniques. The beamline is split in two branch lines serving at the moment three end stations, with a possibility of adding a fourth station at the reserved open port. The optics is similar for both branch lines, providing either focussed or defocussed beam on sample. The Surface and Material Science (SMS) branch hosts essentially experiments on solid surfaces at ultra-high vacuum (UHV) conditions, while the Low-Density Matter (LDM) branch is mainly foreseen for experiments on volatile targets at somewhat higher pressures.

The first (permanent) end station EA01 (where "E" stands for "end station", "A" is the A-/SMS- branch, "01" means the first station from the ring) offers high-resolution ultraviolet PES (UPS), core-level x-ray PES (XPS) and near-edge x-ray absorption fine structure (NEXAFS) spectroscopy in several detection modes. While targeting mainly core-level studies, the station has capabilities for measuring valence band structures with angle-resolved photoemission (ARPES). This station is a deeply refurbished version of a surface science station transferred from the MAX II ring at MAX-lab; it is in user operation from February 2020.

The second (permanent) end station EB02 (B- or LDM-branch) is focussed primarily on PES studies in liquid, molecular and free cluster jets, but can also be used for investigations of solid samples, especially non-UHV compatible ones. The station enables a rapid exchange of a variety of different sample delivery systems / jet sources belonging to the MAX IV LDM community. This station was also transferred from the MAX II ring at MAX-lab, it is now upgraded and put in user operation since February 2020.

The third (mobile) end station EB01 or ICE ("Ions in Coincidence with Electrons") features a reaction microscope (REMI) for multi-coincidence experiments on volatile targets. This is a new station designed to be compatible with a number of MAX IV LDM-relevant beamlines. The first general user experiments will be performed with the ICE REMI in autumn 2022.

FlexPES was designed as a general-purpose soft x-ray beamline featuring up to four end stations with different sample environments and beam focussing conditions, capable to attract diverse user communities, and capable to evolve quickly to match the advancing user demands. Due to economic reasons, this beamline was a part of the so-called Transfer Package Project upon the transition from the predecessor MAX-lab to the present MAX IV, which resulted in re-furbishing and re-using selected key components from several old beamlines: the x-ray source, the monochromator and (partly) the two end stations. Despite the record-low construction budget, all design goals were achieved, and the entire scope of the planned instruments and techniques was delivered.

We believe the following are the overall strengths of the FlexPES beamline:

- High energy resolution at a decent flux over a wide energy range
- Possibility for focussed and defocussed beam on sample
- Variety of detectors and sample environments
- Continuous/fast/non-stop energy scanning
- High level of automation and ease of operation

Although the baseline operation level is achieved in all our setups, further developments are either ongoing or planned or discussed for exploiting the full potential of the beamline, as detailed in the section “Developments”.

FlexPES was constructed with a budget of 31 MSEK or ca. 3 MEUR. Today it operates on the annual budget around 400 kSEK (ca. 38 kEUR) with the possibility to apply additionally for internal upkeep grants for smaller upgrade projects. Staff salaries and travel expenses are covered separately.

Although our efforts have already converted in high interest among user communities, on the horizon of 2-3 years our ambition is to increase user satisfaction and broaden beamline capabilities. This shall be achieved by realizing several upgrade projects, further developing automation routines and further optimizing our support practices. On the other hand, already today the “healthy” oversubscription numbers of 2 to 3 are reached. In this context, further improvement in the beamline performance is essential for boosting the quality of the scientific outcome, but it will hardly facilitate user access to FlexPES, rather the opposite (due to increased competition). Although it may be too premature after two years of operation to discuss whether and how the experimental throughput can be increased, some strategical routes can already be considered, as discussed in Section “Developments”.

2 Technical description

2.1 Beamline design

The optical beamline design was primarily performed by Alexei Preobrajenski, using the XRT software package[1] written by Konstantin Klementiev, both MAX IV. The design had to accommodate the undulator and the monochromator used in the past at different MAX-lab beamlines; it had to solve adequately the heat load issues, use the floor space efficiently, enable a variety of focal points for end stations, and provide high energy resolution at relatively high flux within a broad energy range and with an option of both focussed and defocussed beam on sample. In the following sections we will describe the source and the optics of FlexPES and illustrate the beamline present performance. For in-depth reading about the design principles and solutions we refer to the following two documents. The “Detailed design review” (Appendix I) is describing the entire FlexPES project, while the “Detailed optical design report” (Appendix II) is focussed specifically on the optics. Notice that these documents were written essentially in 2015, and some aspects of the design have changed considerably, especially the end station chapter.

[1] K. Klementiev et al., Powerful scriptable ray tracing package xrt, https://doi.org/10.1117/12.2061400

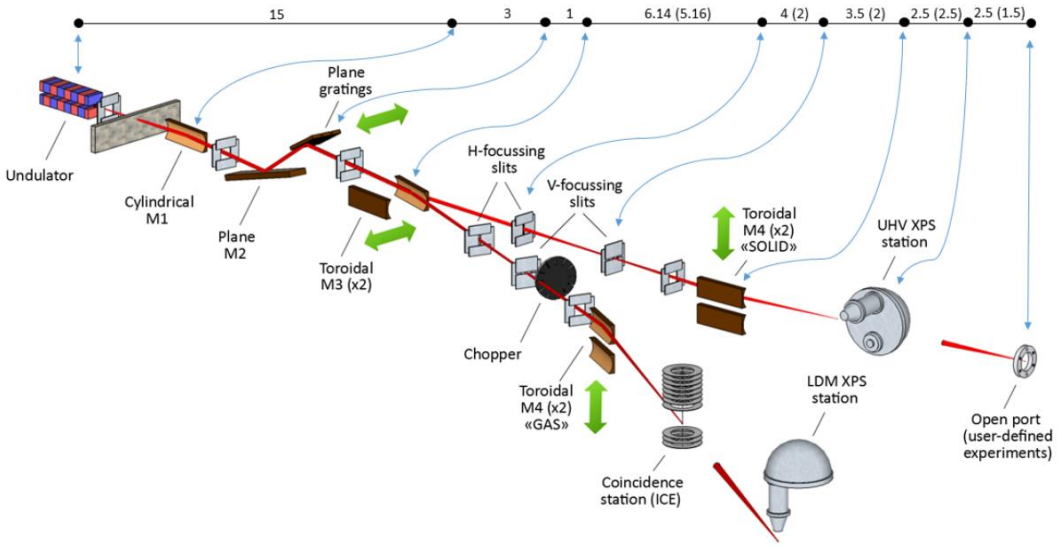

Fiigure 2.1: FlexPES beamline layout with optical elements depicted. Distances are given on top in meters; values without (in) parenthesis correspond to the SMS (LDM) branch.

2.1.1 1.5 GeV ring and insertion device

The MAX IV 1.5 GeV electron storage ring is based on a compact double-bend achromat lattice for the production of bright soft x-ray and UV radiation. With its circumference of 96 m and 12 achromat sections, it is using the same magnet technology as the 3 GeV ring, providing very low (for its energy range) emittance of the electron beam. This is an excellent prerequisite for designing beamlines with small and bright x-ray sources. At the centre of the FlexPES straight section, the RMS values of the e-beam size and divergence are 184 (h) x 13 (v) um and 33 (h) x 5 (v) urad, respectively. The 1.5 GeV ring operates today with the current of 400 mA and top-up period of 30 min. Once per semester single bunch delivery is provided for users from both the LDM and photoluminescence community. In that mode, the current is ~23 mA and a top of period of 30 min to 2 hours is possible on request.

The linearly polarizing undulator (LPU) U54.4 from the beamline I311 at MAX-lab was used as the x-ray source for FlexPES. It has 49 periods, period length of 54.4 mm, effective vertical field of 0.85 T and effective K-value of 4.315. With its minimal gap of 16 mm, it can deliver photon energies starting from 38 eV (practical limitation set by the monochromator is around 43 eV). This LPU can also be tapered for broadening the undulator harmonics (whenever a more monotonous spectrum is desirable). Although stemming from late 90s, the device is in good working shape. It got new magnets in 2010 and its magnetic structure was fully characterized prior to the installation. It was also equipped with new motors, encoders and sensors, and integrated into the general control system of MAX IV. Figure 2.2 (a) shows the brilliance of this source in a straight section of the MAX IV 1.5 GeV ring for

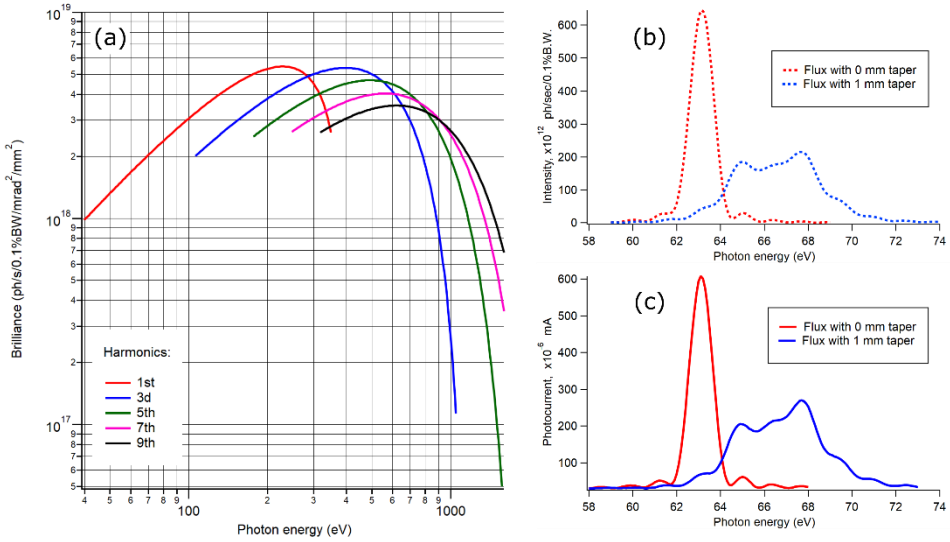

***Figure 2.2**: (a) Brilliance distribution of synchrotron radiation from the FlexPES LPU with 500 mA in the ring and using 0.1% band width of the monochromator. (b) Calculated undulator spectra (first harmonic) for the gap of 20 mm and the acceptance cone of 100x100 urad2 in the case of straight (red) and tapered (blue) magnet arrangement. (c) The same as (b) but measured experimentally.*

the five harmonics we are using in the entire photon energy range, as calculated under the assumption of 500 mA in the ring. The performance of the insertion device was characterized after the beamline alignment and energy calibration by measuring the undulator spectra and comparing them with the results calculated using the SPECTRA software[2]. A variety of spectra were recorded with different energies, harmonic numbers, beamline acceptance and tapering conditions, all showing good correspondence between the measured and the calculated spectral shapes. As an example, Figure 2.2 provides a comparison of the predicted (b) and measured (c) undulator spectra of the first harmonic for the on-axis radiation conditions and the gap of 20 mm.

Although the present LPU is in good shape, the physical aging of the mechanics and the magnets, as well as the lack of full polarization control, represent a problem for the future operation and further beamline development. An upgrade of this device with a more modern and versatile undulator should be considered, and some ideas for this upgrade are presented in “Developments”.

2.1.2 Beamline optics

After passing the frontend, the LPU radiation is deflected horizontally (by 4°) and collimated vertically by a water-cooled cylindrical mirror M1. The size of its optical area is defining the ultimate beamline acceptance of 0.62 (h) x 1.36 (v) mrad. For practical reasons (easier handling of the heat load) we reduce this acceptance further with the frontend masks, but the irradiated footprint on M1 remains sufficient to accept 99% of the desired monochromatic radiation. Prior to entering the monochromator, the acceptance can be further reduced by the water-cooled beam-defining apertures.

The Zeiss SX-700 plane grating monochromator (PGM) re-used from the former beamline I511 at MAX-lab is operating in the collimated PGM scheme. With this scheme, the beam is parallel to the floor (i.e., easier operation and exchange of end stations), the resolution is less sensitive to the slope errors on

[2] T. Tanaka et al., SPECTRA: a synchrotron radiation calculation code, J. Synchrotron Rad. (2001). 8, 1221

optical elements, and the exit slit is fixed in space for different c_{ff} values (the PGM parameter c_{ff} is a cosine ratio of the diffracted and incident angles, and may be varied for better suppression of the higher diffraction orders). Before installing at FlexPES, our SX-700 was equipped with new stepper motors, drives and gear boxes; it also was integrated in the standard MAX IV control system and calibrated. The optical elements inside the monochromator are the plane mirror (M2) and the plane gratings (PG, up to three). The old optical elements have been preserved but cleaned; the reflectivity of the main (1221mm^{-1}) grating has been characterized at BESSY (Berlin) and found acceptable. The overall performance of the PGM after the refurbishing is quite satisfactory. We have recently implemented measurements in the continuous scanning mode, which implies precise motion of M2 and PG along certain trajectories, and the monochromator demonstrates highly accurate and reproducible behaviour in this regime. Currently only one grating (1221mm^{-1}) is in use for the entire energy range, while the second one (400 mm^{-1}) has been recently manufactured, characterized and installed (commissioning ongoing). This second grating should greatly increase the flux in the low-energy range (below 150 eV), which is highly desirable e.g., for ARPES. The characteristics of the presently available gratings are summarized in Table 1. With the new 400 mm^{-1} grating covering low-E range, it would be good to optimize the performance of the main grating towards higher energies by manufacturing a new one, see Section "Developments".

Table 1: Characteristics of gratings installed at FlexPES.

	Groove density (l/mm)	Optical area (mm)	Substrate	Coating	Slope errors (arcsec)	Blaze angle (°)
PG1 (main)	1221	110 x 30	Si	Au	0.1 / 0.1	1.35
PG2 (new)	400	110 x 30	Si	Au	0.04 / 0.04	1.55

A pair of toroidal mirrors M3a and M3b (one at a time, switchable) are focussing the radiation onto exit slits in the SMS- and LDM-branches, respectively. The intermediate focus is made astigmatic on both branches, with the horizontal focus preceding the vertical one. The stronger focussing in the horizontal plane allows elongating the entrance arm on the next (refocussing) mirrors, M4a and M4b, in the same plane, thus increasing the demagnification in horizontal direction and improving the aspect ratio of the beam spot at the sample (making it less elongated horizontally). Each slit (two horizontal and two vertical) can be controlled in width, and their position along the beam can be adjusted to compensate for a misalignment and mirror shape errors. This adjustment is essential for achieving theoretical values of resolution and spot size. After the exit slits, both branches are equipped with gas cells for monitoring beamline resolution with the spectra of gases (e.g. He, N_2 and Ne).

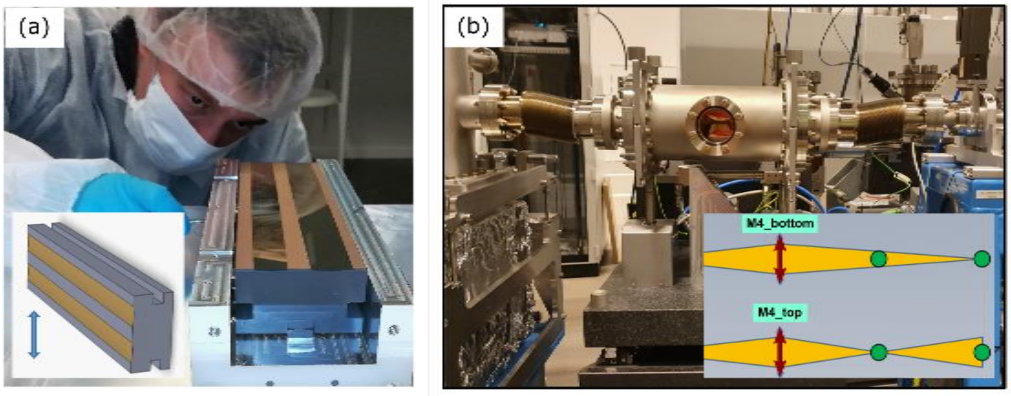

***Figure 2.3**: (a) Installing one of the twin-toroid M4 mirrors on its holder; inset shows the M4 geometry and motion directions in UHV. (b) M4 vacuum chamber with its granite wedge mechanics for precise vertical translations; inset: schematics of focussing in the two possible focal points.*

Each M4 is manufactured as a pair of toroidal mirror stripes with different curvature placed on the same substrate (Figure 2.3, a). Each stripe can be selected by moving M4 up or down; they are deflecting the beam horizontally and are focussing it on the sample: one stripe into the first end station, another one – into the second (Figure 2.3, b). In this way, we can accommodate two different experimental setups on each branch without an additional re-focussing in-between. As an important bonus, this arrangement allows us to either focus or defocus the beam on the sample, depending on the sample type and sensitivity to the radiation damage. This feature is highly appreciated by many users at FlexPES. The overall beamline layout and all critical distances are shown in Figure 2.1. Characteristics of the mirrors are summarized in Table 2.

Table 2: Mirror parameters in the FlexPES beamline.

	M1	M2	M3a / b	M4a_1 / a_2	M4b_1 / b_2
Shape	cylindrical	plane	toroidal / toroidal	toroidal / toroidal	toroidal / toroidal
Deflection	hor.	vert.	hor. / hor.	hor. / hor.	hor. / hor.
Distance (m)	15	variable	19	32.5 / 32.5	28 / 28
Incidence angle (°)	2	1 - 13	2	2 / 2	2 / 2
Block size (mm)	300 x 40 x 60	640 x 40 x 110	260 x 40 x 40 / 260 x 40 x 40	260 x 75 x 40	260 x 75 x 40
Opt. area (mm)	280 x 20	640 x 40	240 x 20	two stripes of 240 x 20	two stripes of 240 x 20
Substrate material	Si	Si	Si	ZERODUR®	ZERODUR®
Coating material	Au	Au	Au	Au / Au	Au / Au
Roughness (Å)	3	3	3	5 / 5	5 / 5
RMS slope error, tang. / sag. (arcsec)	0.08 / <1	0.1 / 0.1	0.23 / <1 0.13 / <1	0.19 / <1 0.14 / <1	0.23 / <1 0.26 / <1
RMS radii tang. / sag. (mm)	∞ / 1047	∞ / ∞	271278 / 698 238740 / 489	107935 / 102 175101 / 143	76410 / 70 114615 / 93

Motorized diagnostic sections on each branch allow us to measure 1) the profile of the beam at M4 with YAG screens and cameras and 2) the total photon flux with photodiodes. These tools were used extensively for the beamline alignment, and are still used occasionally for the performance checks. Particularly important for the regular user operation are the I_0 sections placed at the end of each branch just before the end stations. We use an Au foil with an opening (slit for the beam) as an I_0 sensor and evaporate fresh gold on it regularly to keep it contamination-free. Clean I_0 signals are absolutely essential for delivering high-quality NEXAFS data. Other diagnostic tools are phosphorus screens and cameras on the 1) beam-defining apertures before the PGM, 2) beam-defining apertures before M3 and M4, and 3) exit slits. Finally, we are constantly monitoring the drain current from both M4 mirrors.

On the LDM-branch, an x-ray chopper is permanently installed immediately after the exit slit, which can be used to increase the separation between x-ray pulses (for e.g. ToF measurements) during single-bunch operation of the 1.5 GeV ring (see Figure 2.4). This is necessary when using e.g., a magnetic bottle spectrometer to measure electrons over a broad kinetic energy range and can also be useful for studying e.g. particle fragmentation processes involving heavy ions with low velocities (typical LDM relevant experiments). The design of the chopper was developed at Uppsala University and is based on a rotating disc with slits at the disc perimeter, mounted on a magnetically levitating bearing. The opening time of the chopper is defined by the rotation speed of the disc, its size, the slit width, and the height of the photon beam. To guarantee that only a single x-ray pulse can pass, the opening time of <300 ns is needed (pulse period in the single bunch mode is 320 ns). At a rotation speed of ≈0.8 kHz and a disc diameter of 240 mm, this would require the sum of the beam height and

the disc slit width to be less than ≈180 µm. Therefore, a slit width of 85 µm in the disc and a fixed horizontal slit with a width of 85 µm just in front of the disc (to limit the beam height) were selected. The vertical focus of the M3 mirror is at the exit slit, and the beam diverges after this point, meaning the fixed slit and the disc slit will cut the beam to some degree. The transmission is around 65 % for the small exit slits (<85 µm) and decreases for larger slit settings. The speed and phase of the disc rotation is controlled by a MAX IV-designed closed loop control system, which uses the ring bunch marker and the signal from a fast photodiode illuminated by a laser on the other side of the disc, generating a pulse every time a slit passes by, as input. We can thus synchronize the chopper to the x-ray pulses, dramatically increasing its efficiency, and additionally allow lower rotation speeds without risking multiple pulses in the open time. The chopper is positioned into the beam by a linear translation on rails, with high reproducibility. The chopper will be offered to users from autumn 2022. The FinEstBeAMS chopper design is based on the FlexPES solution and is intended to be ready in 2023.

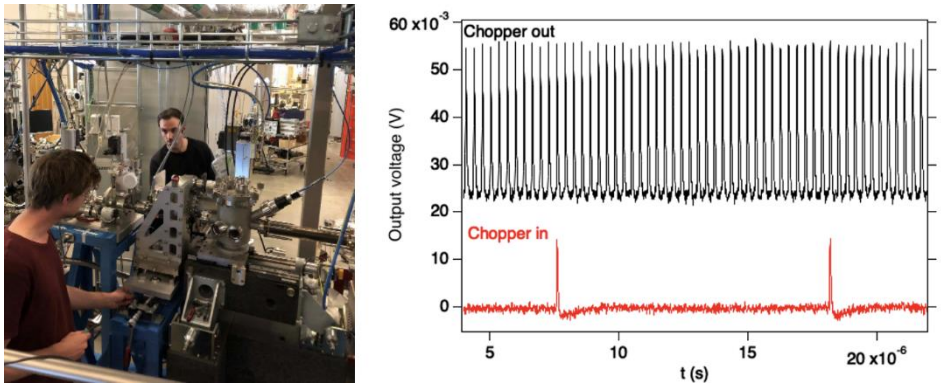

***Figure 2.4**: Left: Chopper being installed by the MAX IV alignment team. The cylindrical chamber on the right houses the exit slit, and the chamber immediately to the left houses the chopper. Right: x-ray pulses in the single bunch mode measured with a photodiode at EB01/ICE; top chopper out, bottom chopper in. The period of the x-ray pulses increases from 320 ns to 10.56 µs with the chopper in. The transmission for this slit setting (170 µm) is ≈40%.*

2.1.3 Measured vs calculated performance

Energy resolution. The energy resolution of the beamline was characterized and optimized by collecting and analysing NEXAFS spectra of gases in the gas cells at both branches, with the typical gas pressure around 5 x 10^{-4} mbar. The most useful for extracting resolution figures in our photon energy range are He, N_2 and Ne, but additional characterization was performed also with the spectra of Ar, Kr and Xe. The calculated results shown below for comparison are obtained with the real (not ideal) beamline raytracing, including imperfections of optical elements, real magnetic fields in the LPU and angular acceptance used in practice.

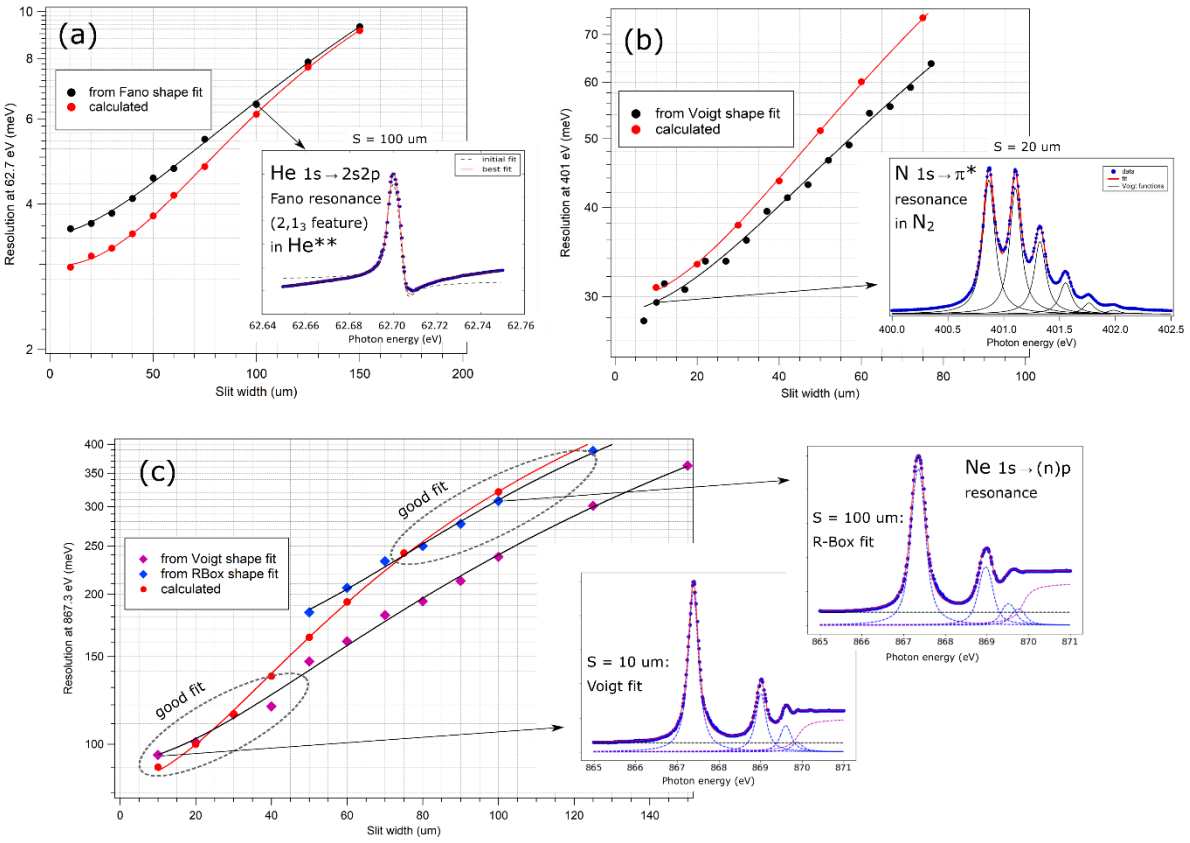

***Figure 2.5**: Energy resolution ΔE (FWHM) at the SMS branch determined from the spectra of different gases and compared with the raytracing calculation results. (a) @ 62.7 eV, with the help of the $2,1_3$ Fano resonance in He (inset: He spectrum, exit slit 100 um), (b) @ 401 eV, with the help of the 1s→2p(π*) resonance in N_2 (inset: N_2 spectrum, exit slit 10 um), (c) @ 867.3 eV, with the help of the 1s→3p transition in Ne (inset: Ne spectra taken with the slits 10 and 100 um and fitted with Voigt profiles and rounded box profiles, respectively).*

At lower energies, the $2,1_3$ autoionization resonance in double ionized He at 62.7 eV was used for estimating the energy resolution, which can be determined by fitting this feature with a Fano shape profile as shown in Figure 2.4 (a, inset). The systematic fit of the spectra (c_{ff} = 2.25, 1221 mm^{-1} grating) with increasing exit slit width provides a reliable estimate of the resolution figures, with the best measured value of 3.5 meV at this photon energy. It is marginally worse than the theoretical prediction of 3.0 meV, and the discrepancy gets even smaller with increasing slit width (see Figure 2.5a).

For the middle energy range, the vibrationally resolved N 1s→2p(π*) resonance in N_2 at ~401 eV is a convenient fingerprint of the resolution (see Figure 2.5b, inset). We fitted all peaks by Voigt functions with the fixed Lorentzian width of 120 meV (average of several literature values), and averaged the obtained Gaussian broadening over the first four (most intense) peaks. As seen in Figure 2.5b, the measured resolution figures are even slightly better than the predicted values (which may be due to slight overestimation of the lifetime broadening used in the fit). This trend is consistent for a wide range of exit slit widths providing confidence in the fitting results.

At higher energies, the Ne 1s→np (n=3, 4, 5, …) progression in neon gas was used for estimating the beamline resolution. All individual transitions were fitted with either Voigt or rounded-box spectral shapes, and the Gaussian FWHM was obtained from the deconvolution of the 1s→3p peak at 867.3 eV in the assumption of its Lorentzian lifetime broadening of 260 meV[3]. It turned out that the Voigt shape fit works best for the smaller slit widths (below 40 um), while the rounded-box shapes were

[3] M. Coreno et al., Phys. Rev. A 59, 2494 (1999).

necessary for the correct fit at larger openings (above 50 um), as shown in Figure 2.5 (c). Also at these energies, the correspondence between the measured and the expected resolution is excellent.

The energy resolution examples shown in Figure 2.5 are specific for the SMS branch, but the same analysis was performed for the LDM branch as well. Due to shorter distances between optical elements, the same slit openings result here in slightly worse resolution and slightly higher flux, but the trends with varying energy and slit width are identical with the SMS branch and match the expected behaviour equally good.

In practice, the in-house developed resolution calculating software provides users with the beamline resolution as a function of energy and slit opening, and also calculates the photoelectron analyser resolution, and the total resolution.

Energy scale and scanning. For energy calibration the offsets of optical elements in the PGM were adjusted first to ensure zero energy shifts with varying c_{ff} values[4]. After that, the energy scale is calibrated individually for each branch using the Fermi level positions measured from a clean Au sample. The accuracy and reproducibility of the energy scale is within 100 meV below 500 eV but deteriorates at higher energies (up to 0.5 eV at around 1500 eV). The energy can be scanned either in the standard step-by-step regime or continuously. XAS spectra recording in the non-stop scanning mode involves a complex trajectory motion of the optical elements and the LPU combined with trigger-based acquisition with a number of detectors. FlexPES has pioneered this scanning mode at MAX IV, and now we can scan on average 5 to 10 times faster than in the stepwise mode without losing any spectral quality (rather the opposite).

Flux. The absolute photon flux measurements were performed with the silicon photodiode (AXUV 100 from IRD) positioned after the refocussing optics. The same angular acceptance of 124 (h) x 62 (h) urad (corresponding to the most typical mode of a narrow on-axis radiation cone), the 1221 mm^{-1} grating and the c_{ff}=2.25 were used both in the measurements and in the raytracing. At FlexPES the LPU gap motion is synchronized with the PGM motion, and the flux curves were recorded using energy scanning across harmonics 1, 3, 5, 7 and 9 for different energy intervals. An example of the resulting flux curves in the entire energy span is shown in Figure 2.6 (a). The "raw" measured curve is normalized to the responsivity of the photodiode and to the photon energy (as the current production in the photodiode is proportional to it). As can be seen, the overall shape of the measured curve is very similar to the expected behaviour, with the C 1s and O 1s absorption features being absent in the calculated curve. The measured flux is lower on average by a factor of 2, but we consider the agreement with the raytracing result very satisfactory, as too many details can affect the absolute flux measurements: somewhat different magnetic field in the LPU, somewhat different grating efficiency, somewhat different beam acceptance, as well as the presence (even small) of C- and O-contaminations. The flux on sample is increasing strictly linearly with the opening of the exit slit, as shown in Figure 2.6 (b), as a sign of good alignment. The characterization of the flux and resolution with the new 400 mm^{-1} grating is ongoing, but the first flux measurement is shown in Figure 2.6 (a, blue curve). As expected, this grating gives a gain by factor 5 to 10 in the low-energy range (at the cost of ca. 3x worse resolution).

[4] M. R. Weiss et al., Nuclear Instruments and Methods in Physics Research A 467, 482 (2001).

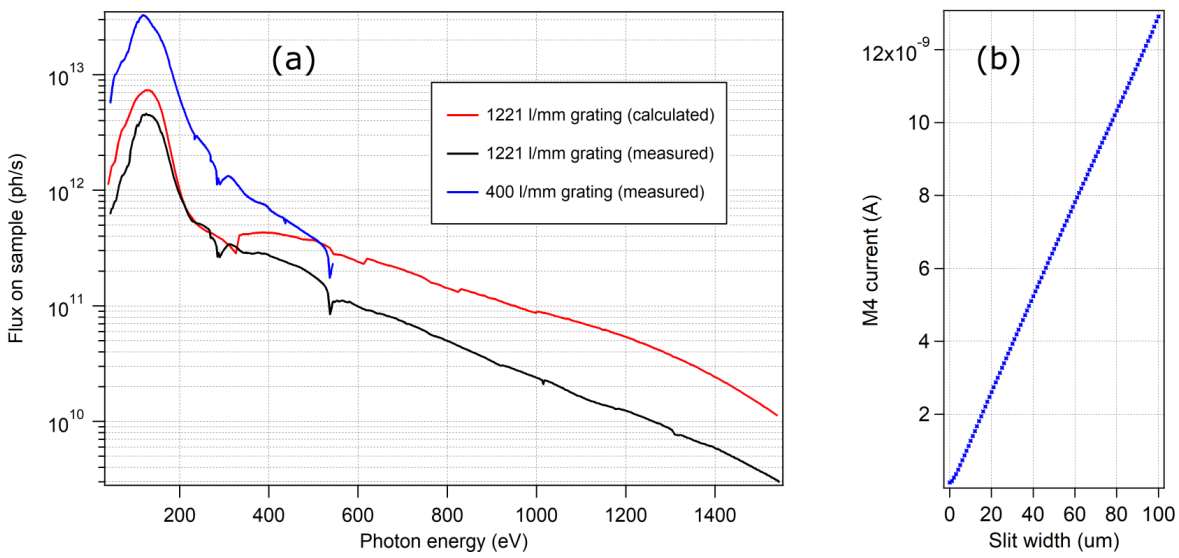

***Figure 2.6**: (a) Black curve: photon flux for the entire energy range, measured at sample on the SMS branch with the exit slit of 20 um, 1221 mm^{-1} grating, c_{ff}=2.25 and angular beamline acceptance of 124 (h) x 62 (h) urad and scaled to the intended final stored current of 500 mA (400 mA today). Red curve: raytracing calculation with the same parameters. Blue curve: measurement with the same parameters with the new 400 mm^{-1} grating. (b) Measured beam intensity (M4 current) as a function of the exit slit opening.*

Spot profile. At FlexPES there are in total four secondary focal points (two on each branch), and in each point the spot can either be focussed or defocussed. We have characterized spot profiles in all focal points by using a custom-made YAG screen with a fine mesh and a long-focus microscope. In general, all results are perfectly matching the raytracing calculations. As an example, in Figure 2.7 we show photographs of the beam at the sample position in the first end station on the SMS branch (EA01 station). The focussed beam profile is shown in Figure 2.7 (a) (E = 265 eV, LPU gap 40 mm, horizontal exit slit 150 um, vertical exit slit 20 um), where it is compared with the corresponding raytracing result. The same profile with FWHM of 50 (h) x 15 (v) um is observed. For the given slit openings, this size simply reflects the demagnification of the intermediate focus by the factor of 3 (1.4) in the horizontal (vertical) plane and can be reduced further by closing the slits. The defocussed beam in the same point has the size/FWHM of 1 (h) x 0.4 (v) mm for the on-axis radiation (Figure 2.7, b) and can be modified to the donut-shape by using off-axis radiation (Figure 2.7, c), although this is rarely used in practice. The origin for the appearance of the on-axis and off-axis radiation is illustrated in the calculation in Figure 2.7 (d). In the other focal points, the maximum horizontal size of the focussed beam spot is: 100 um (SMS branch, 2nd point), 70 um (LDM-branch, 1st point) and 130 um (LDM-branch, 2nd point).

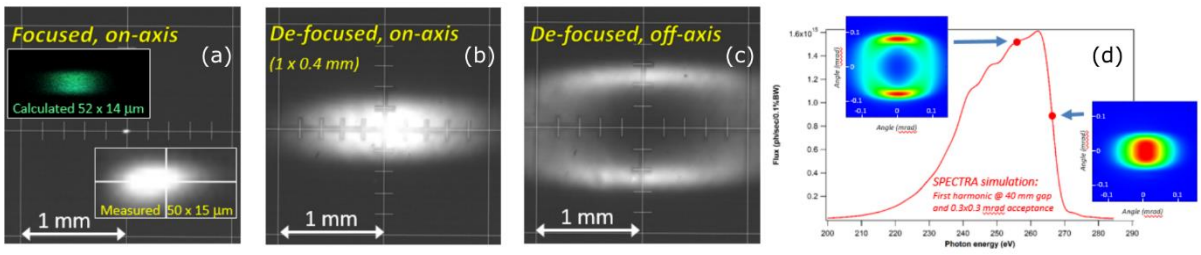

***Figure 2.7**: (a-c) Beam spot at the sample photographed in the EA01 end station; E = 265 eV, gap 40 mm, slits 150 (h) x 20 (v). (a) Focussed beam, compared with the raytracing result, (b) defocussed beam, on-axis, (c) defocussed beam, off-axis. (d) Calculated spectrum of the 1st LPU harmonic for the large (0.3 x 0.3 mrad) angular acceptance; insets show angular distributions of the monochromatic beam taken at different energies of the spectrum.*

Status of optics. Already within the 1st month of active beamline commissioning the surfaces of all optical elements were heavily contaminated with carbon, so that the measured intensity loss at the C 1s absorption dip at 284 eV was close to 100%. This problem was dealt with by creating several gas insertion points along the beamline for dosing molecular oxygen. In the presence of white (UV) light molecular oxygen gets activated and can attack C contaminations efficiently. After the prolonged cleaning we could reduce the beam losses (as measured between M3 and M4) to zero and use now a small O2 pressure in the M1, PGM and M3 chambers all the time. This keeps the M1, M2 and the grating permanently clean. However, as M3 and M4 do not normally see any UV light, they remain contaminated, and need intentional regular cleaning with the zero-order light and O_2. As no time with beam is foreseen specifically for the cleaning purposes (and many hours or even days are needed to get mirrors perfectly clean), the cleaning can only be performed occasionally. As a result, we normally have to compromise by using slightly contaminated M3 and M4, with the beam loss of some 20-30% at the C absorption dip of 284 eV. One also should be careful with oxygen, as prolonged exposures may result in the oxidation of the substrates of optical elements and produce dips at the O 1s edge. As for the I_0 monitors, they get fresh Au coatings regularly, and their signals can be safely used for the signal normalization.

2.2 The A-branch end station EA01: XPS and NEXAFS on surfaces in UHV

2.2.1 Overview

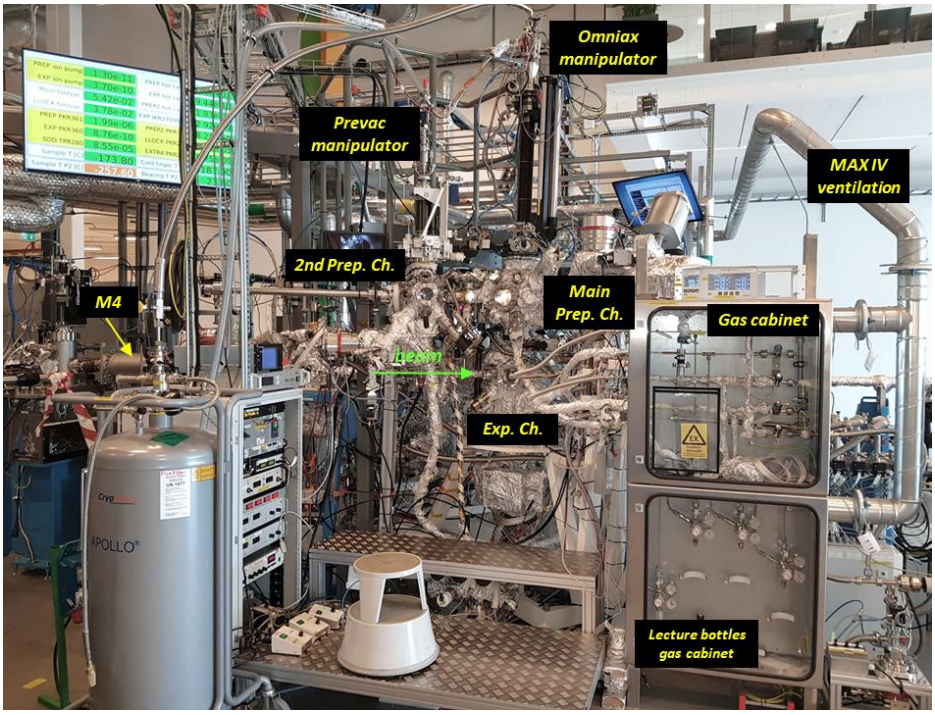

***Figure 2.8**: EA01 end station with peripheral equipment.*

The permanent end station EA01 is designed for studies of electronic properties of surfaces, interfaces, 2D materials and thin films in UHV conditions; it is serving communities of the surface and the material scientists, primarily from Sweden and Europe. The set of techniques includes a combination of XPS, UPS, NEXAFS spectroscopy, resonant PES, secondary electron cut-off measurements, and (to some extent) ARPES. The NEXAFS technique is implemented in several detection modes with different surface/bulk sensitivity, including total, partial and Auger electron yield modes (TEY, PEY, and AEY) and partial fluorescence yield mode (PFY). As a recent development, the TEY, PEY and PFY detection modes are enabled simultaneously in a continuous scan regime,

allowing us to record the NEXAFS spectra on average 5-10 times faster than in the step scan mode. The end station layout is based on the well-proven design concept used previously at the D1011 beamline of the MAX II storage ring, although all vacuum chambers and the majority of key components are redesigned and rebuilt to suit user needs in the most optimal way. The most important recent upgrade is the new DA30-L electron analyser (from ScientaOmicron) along with the new µ-metal analysis chamber, which were installed in July 2021 and commissioned in September 2021. The 4-axis Omniax manipulator from VACGEN is the only major part inherited from the old lab (although fully serviced and in reasonably good shape).

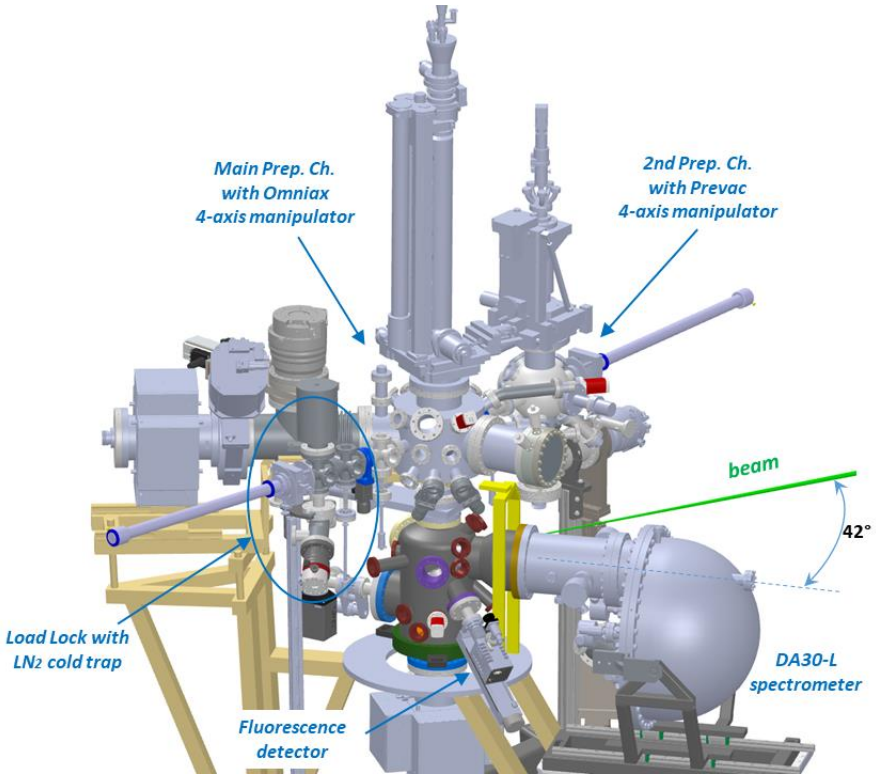

***Figure 2.9**: A 3D CAD model of FlexPES A-branch end station EA01.*

A general overview of the end station and its 3D CAD model are shown in Figures 2.8 and 2.9, respectively. The end station consists of four main chambers. The analysis/experimental chamber houses the DA30-L electron spectrometer and other detectors. The main preparation chamber is placed on top of the analysis chamber. Apart from its main function (sample preparation), it is used for accessing and linking two other areas - a smaller spherical secondary preparation chamber and a load-lock chamber, used for sample loading to UHV. The primary manipulator (VACGEN Omniax) on top of the main preparation chamber can travel down into the analysis chamber for measurements. It is equipped with a new LHe flow-type cryostat (custom-modified Janis ST-400) allowing for a wide sample temperature range from about 20 K up to annealing temperatures as high as 1200 °C. To accommodate this wide range of temperatures, a dedicated sample environment and sample transfer system were developed, which are compatible with the standard flag-type sample holders, slightly adopted for our needs. Samples can be heated either with a hot filament, or by e-beam, or by direct current through the sample. The 4-axis manipulator (from Prevac) at the second preparation chamber has the same heating capabilities, but it has no cryostat and cooling is realized by a recently added heat exchanger. The second preparation chamber is mainly intended for more 'dirty' applications such as organic film deposition, but can also be used for sample preparation in parallel with the

measurements on another sample in the analysis chamber, thus making the beamtime usage more efficient.

2.2.2 Sample holders and transfer system

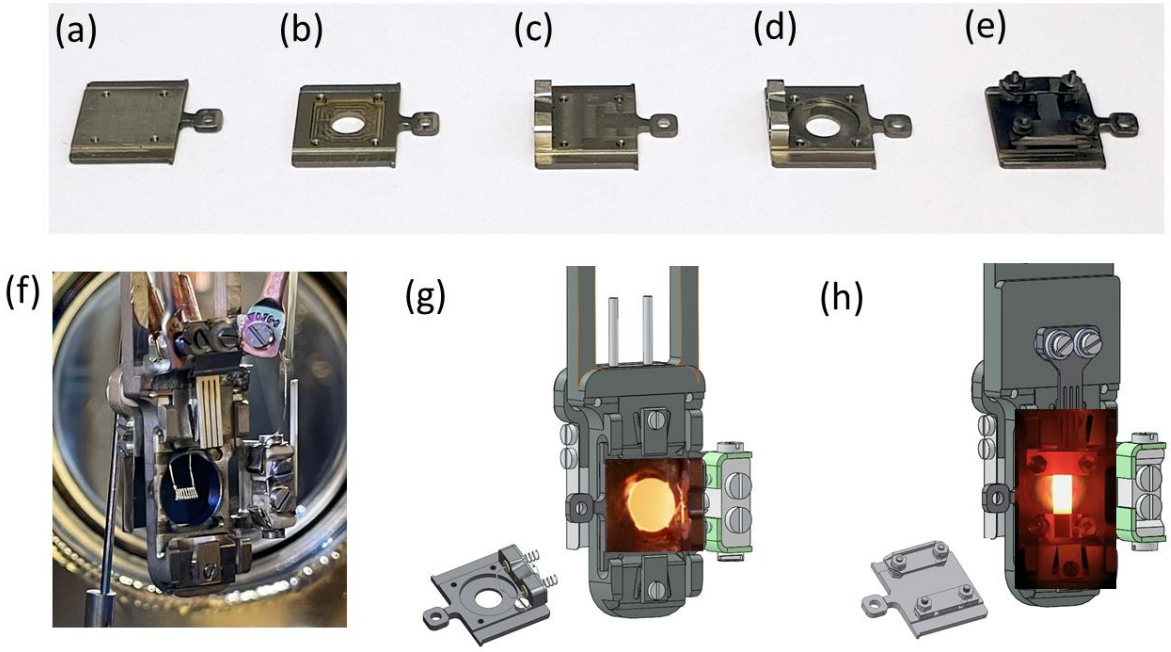

***Figure 2.10**: Mo sample holders used at the EA01 end station: (a)-(b) simple holders without temperature control; (c)-(d) sample holders with possibility to mount thermocouple terminals (ThC not mounted on the photo); (e) sample holder used for direct current heating of samples. Sample recipient part is shown without sample on (f) and with a sample annealed using e-beam heating (g) and direct current heating (h).*

Samples can be mounted on the dedicated holders/plates and placed into different areas of the end station, including sample manipulators and several storage places. All holders are compatible with the Omicron flag-type spades, which is a common standard at most of MAX IV soft x-ray beamlines and the STM lab. This allows for sample transferring to different end stations/UHV setups at MAX IV using a UHV vacuum suitcase. In particular, in-vacuum sample transfer between the MAX IV STM and the EA01 station is a popular feature routinely used by several users groups. There are several different versions of the sample spades (Figure 2.10, a-e) in order to accomplish different user cases and sample preparation procedures. The simplest type – just flat (a) or flat bored (b) holder – does not allow for an accurate temperature control, however provides most space for several samples (commonly up to four). Another type of sample holders, present in several variants (with a bored hole or without), is used for experiments where a precise temperature control is needed, Figure 2.10 (c-d). Thermocouple (ThC) terminals are integrated into these sample holders enabling the ThC to be attached in the very vicinity of the sample surface. In addition, these ThC terminals can be used as extra electrodes for e.g. applying voltage bias across the sample – an option that may be utilized in the future users experiments more (as tested e.g. for in situ ferroelectric switching of prototypic memory devices). On demand, samples can also be heated with the direct current through by placing them on the dedicated holder (Figure 2.10, e).

The sample plates can be loaded from air into the UHV volume through the load-lock chamber. The chamber has a parking stage for loading and storing up to six plates. The stage can be moved out of

the main load-lock volume and separated from it by a manual CF40 gate valve. This is a useful feature for loading moisture-sensitive samples, as they can be loaded in an offline glove box, sealed off by the gate valve and then mounted back on the load-lock chamber. The load-lock can be vented almost instantly using a 'fast vent' macro, which is a part of the machine protection system. The macro logic separates the turbo pump from the vented volume, thus keeping it running non-stop. This automation increases the lifetime of the turbo and speeds up both the venting and the pumping of the load-lock chamber. A typical pump-down time of around 30 min is sufficient to achieve vacuum levels appropriate for further transferring into the UHV volume of the main preparation chamber (below 2E-6 mbar). A LN_2 trap mounted on the load-lock can improve pumping capacity further, if necessary.

Finally, it is worth mentioning that there are six extra sample storage places in each of the preparation chambers (twelve in total). This makes it possible to always keep some samples in UHV in one preparation chamber, while working with higher pressures in the other.

2.2.3 Detectors

The detector arrangement inside the experimental chamber is shown in Figure 2.11. It comprises three main components: an electron spectrometer, a partial electron yield (PEY) NEXAFS detector based on a stack of multi-channel plates (MCP) and a partial fluorescent yield (PFY) silicon-drift NEXAFS detector (SDD).

The electron spectrometer in EA01 is a recently installed hemispherical analyser DA30-L (from ScientaOmicron) with an MCP CCD camera as a detector and lens modes optimized for kinetic energies between 10 and 1500 eV. The analyser lens axis is in the horizontal plane, at 42° with respect to the direction of the incident x-ray beam. The entrance slit of the analyser is horizontal, to better match the spot footprint on the sample (especially for defocussed beam). Our analyser is also equipped with the so-called 'electronic tilt' option using a deflector lens system. Along with the polar angle change on the sample manipulator, the deflector scanning mode enables basic ARPES band mapping with a capability of capturing relatively large segments of the reciprocal space. The analyser resolution was found to follow its specifications and theoretical values for high pass energies, while for smaller pass energies (20 eV and below) one has to assume a presence of extra electronic noise with the magnitude of around 10 meV to match the experimentally measured energy resolution. The source of this noise remains to be identified and eliminated. However, in the most cases it is negligible in comparison with other sources of experimental broadening and the natural width of x-ray core-level excitations.

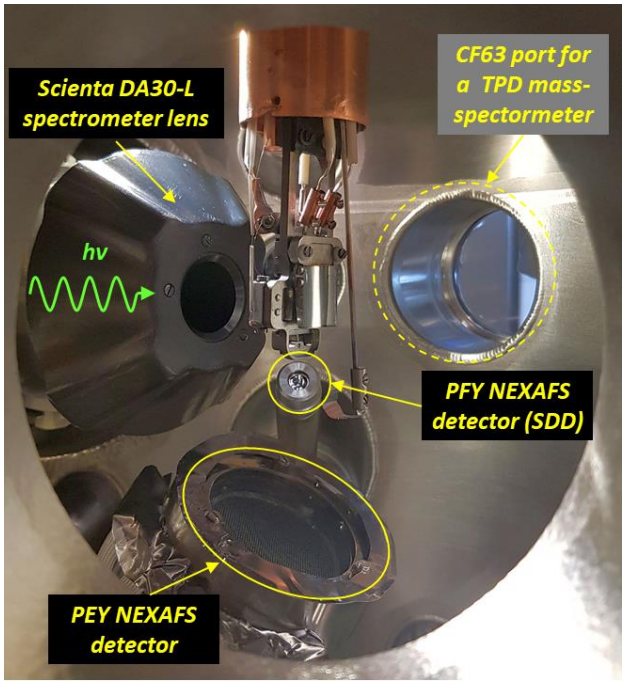

***Figure 2.11**: An overview of the detectors in experimental chamber of the EA01 end station with the sample manipulator in normal photoelectron emission geometry. The monochromatised synchrotron light is coming from the left. The DA30-L spectrometer lens axis is turned away from the beam by 42° in the horizontal plane. NEXAFS fluorescence detector (SDD) is located in the plane perpendicular to the beam and at the 35° angle with respect to the horizontal plane. A CF63 port (135° with respect to the beam) highlighted by the dashed circle is foreseen for temperature programmed desorption experiments with the help of a mass-spectrometer (if funded).*

NEXAFS spectra can be measured in several modes with varying surface/bulk sensitivity. For the electron detection, this includes TEY mode by measuring sample drain current (or in the PEY detector with zero retardation), PEY mode in the home-built MCP detector and Auger electron yield (AEY) mode by means of the DA30-L analyser. Both TEY and PEY currents are detected simultaneously (and together with I_0 signal for normalization) by the MAX IV standard four-channel ALBA electrometer.

For the photon detection, a PFY energy-dispersive NEXAFS detector (SIRIUS®, by Rayspec) is available featuring an SDD with relatively large active area of 70 mm^2, protected by a 70 nm thick silicon nitride window (patented "C2" window from Amptek). The SDD structure has a very low capacitance and provides energy resolution on the scale of 100 eV at relatively short electronic processing times (e.g. 133 eV at 5.9 keV), which is sufficient to isolate an x-ray emission line of interest for the NEXAFS PFY detection. The detector output is going into a digital pulse processor (Xspress-3 mini from Quantum Detectors) capable of accepting high incoming count rates. The PFY mode is the most bulk-sensitive; it is suitable in particular for samples not common for surface science (charging, not too clean or too flat, etc). The main advantage of the partial (for both electron and fluorescence) over the total yield is that it significantly increases the signal-to-background ratio. This is very useful for detecting signals from elements with low concentrations (e.g. sub-monolayers, dilute compounds etc). Although SDD (and alike) fluorescent detectors are a mainstream feature at hard x-ray beamlines, they are not at all common in the soft x-ray regime due to much higher noise and weaker signals. Nevertheless, the PFY-SDD NEXAFS detection mode turned out to be quite powerful and appreciated by our users; FlexPES was the first among soft x-ray beamlines at MAX IV offering it as a standard feature (now also SoftiMAX has implemented a similar detector).

It is worth mentioning that the XAS spectra in all modes, except for AEY, can be recorded simultaneously in a continuous scan manner. The continuous scanning mode has been just recently implemented at FlexPES (also first and so far the only one among soft x-ray beamlines at MAX IV) and resulted in a great reduction of the scan time, usually on the order of 5-10 times in comparison with the technically more simple step-scan mode.

The setup of all detectors (as well as temperature control, operation of sputter guns and leak valves, etc) can mostly be done remotely from the control room, using software developed by the beamline staff in collaboration with the MAX IV KITS (IT support) group. The software highly increases the convenience and safety for users as well as protects the hardware from any improper operation.

Finally, a general KITS project on integration of hemispherical analysers' software in the Tango control system of the beamlines has recently been started. The custom-made control software will enable designing more versatile and fully automated photoemission experiments involving e.g. complex sample trajectory motion, integration of sample temperature or gas pressure in the measurement sequence, etc. In addition, this software shall facilitate adopting .h5 data storage format and standardizing data handling. The FlexPES staff is actively collaborating with the KITS team on the software development and testing.

2.2.4 Sample preparation and characterization

Samples can be prepared in-situ in the main and the secondary preparation chambers with rather similar facilities. This duplication in the sample preparation toolbox increases the overall system redundancy and allows for more efficient time use when working on several samples preparations simultaneously. Both chambers have equipment for standard surface science related experiments, such as ports for evaporators, electrospray sources, UV-lamps, deposition monitors or other user-specific extra equipment, leak valves to introduce gases (some automated, some manual), ion sputter guns (Prevac IS40-C) and cooling/heating capabilities. The evaporator ports are gated and equipped with individual pumping lines to facilitate using such devices without breaking vacuum. The main preparation chamber has also an RGA mass spectrometer (MKS Microvision2), a quartz thickness monitor (Prevac TMC13 controller) and a LEED optics (BDL800 from OCI).

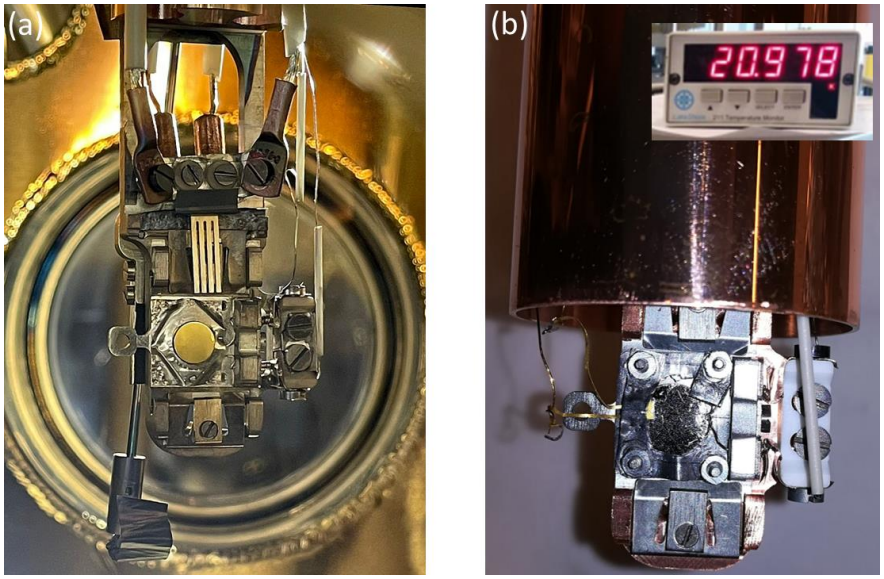

***Figure 2.12**: Examples of the recipient parts for sample manipulators used in the A-branch end station. (a) A recipient part made of Mo with a gold crystal mounted. (b) A recipient part made of Cu with a nickel crystal on the Mo sample holder; the lowest tested sample temperature is 21 K as measured by a Si-diode mounted directly on the sample surface. For a better cooling the cryo-shield (a copper cylinder above the sample holder in (b)) can be moved down as close to the sample as possible.*

In order to accommodate different user cases, there are two versions of the recipient part for the sample manipulators at FlexPES: the standard head made of Mo (Figure 2.12, a) is optimized for higher temperatures (from around 35 K up to 1500 K), while the second one is made of Cu and can be used for experiments with cryogenic temperatures (minimum tested 21 K) and more efficient cooling (Figure 2.12, b). As by today, the overwhelming majority of the users' experiments in the EA01 end

station do not require the LHe cooling, therefore the Mo-based recipient part is used most of the time. On both manipulators it is possible to heat samples up to 1200 °C either by a combination of filament resistive heating and e-beam heating or by direct current heating through the sample. A compressed air cooling can be used to keep the manipulator end parts as cold as possible during sample annealing at high temperatures, which hampers excessive outgassing around the sample and enables effectively long annealing procedures. A cooling down to about 21 K (LHe) or 90 K (LN_2) in the main preparation chamber can be achieved with the help of a LHe flow-type cryostat. The sample temperature can be steered remotely by means of Eurotherm EPC3000 controllers via a GUI program developed by the beamline team, which allows for a user-friendly control of all relevant parameters (temperature setpoints, ramp speeds, PID parameters, etc). Measurements involving electron detection are possible upon heating samples up to 600 °C.

2.2.5 UHV-dosing gas system

Gas leak valves mounted on the preparation chambers are connected via flexible metallic hoses to the five (more on demand) gas lines located inside a ventilated gas cabinet. The gas cabinet is made of two separated parts (see bottom right part of Figure 2.8). The top compartment hosts a gas panel with buffer volumes, valves, pumping line and (in the future) pressure read-outs. The bottom compartment contains gas pressure regulators and is used for connecting small gas cylinders/lecture bottles to the gas lines. At present, there are individual lines for: O_2, hydrocarbons, CO/CO_2, corrosive/toxic gases such as NH_3/NO_2, and for vapours of liquids, but lines for other gases can also be provided. Additionally there is a separate Ar gas line for sputtering in both preparation chambers. All gas lines can be pumped with a dedicated combination of turbo/forevacuum pumps, fully separated from the other pumping systems. To avoid the start/stop cycles in the turbo, gate valves can bypass it whenever high gas load is expected.

The gases can be introduced in both preparation chambers up to maximum pressures of about 1e-5 mbar. The argon dosing is performed automatically by using a motorized leak valve and a control GUI developed in-house. Combined with a remote control of the sputter gun and the motorized sample manipulator, this enables fully automated Ar-sputtering procedures. This option is very much appreciated by the users. One more motorized and computer-controlled leak valve on the main preparation chamber can be used for an accurate gas delivery of other gases from the gas panel.

For the sake of improved usability and safety of this system, it is planned to be upgraded as a part of major development of the beamline gas-delivery systems. An automatic/semiautomatic control with help of electrical manometers and shutoff valves would greatly enhance the safety and the convenience for users by integrating these components into the beamline's equipment protection system and making macro commands for various gas handling procedures (e.g. gas lines pumping, venting, purging etc.).

2.3 The B-branch end station EB02: XPS on LDM and non-UHV targets

2.3.1 Overview

The end station EB02 (Figure 2.13) is a refurbished setup from the I411 beamline of the old MAX-lab. It has been designed to allow electron spectroscopy on both gas-phase and substrate-supported samples. The core part of this end station has three chambers: The Analysis Chamber, the Preparation Chamber, and the Introduction Chamber. The Analysis chamber is equipped with the Scienta R4000 electron energy analyser and can be rotated around the beam direction without breaking vacuum. In this way the angle between the analyser and the photon polarization plane can be selected by the user. Multiple ports of up to CF160 size facilitate mounting of modular setups on the Analysis Chamber – for the in-situ delivery of volatile samples, as described below. The Preparation Chamber has a CF160

door with a view port for direct inserting of solid samples as well as multiple smaller ports for mounting user-specific evaporators and gas dosing. For transferring solid samples, a 600 mm z-travel VG Omniax XYZR manipulator is attached to the preparation chamber along the light axis. The molybdenum sample receiver mounted at the tip of the manipulator rod is designed to accommodate standard flag-type sample plates and allows positioning supported samples at 45° to the light incidence angle. User-specific sample heads can replace the molybdenum receiver on demand. All four manipulator axes are motorized and equipped with absolute encoders for micrometre accuracy and reproducibility. The Introduction Chamber facilitates sample loading, storage and manipulation. It has a CF100 load lock with a view port and a sample storage carousel for 8 flag-type sample. A magnetic transfer arm mounted at 90° to the preparation-chamber manipulator enables sample transfer from the carousel to the receiver head of the Omniax manipulator.

The three chambers of the EB02 end station are separated from each other by gate valves, and each chamber has its own pumping system based on turbo-pumps and dry forevacuum pumps.

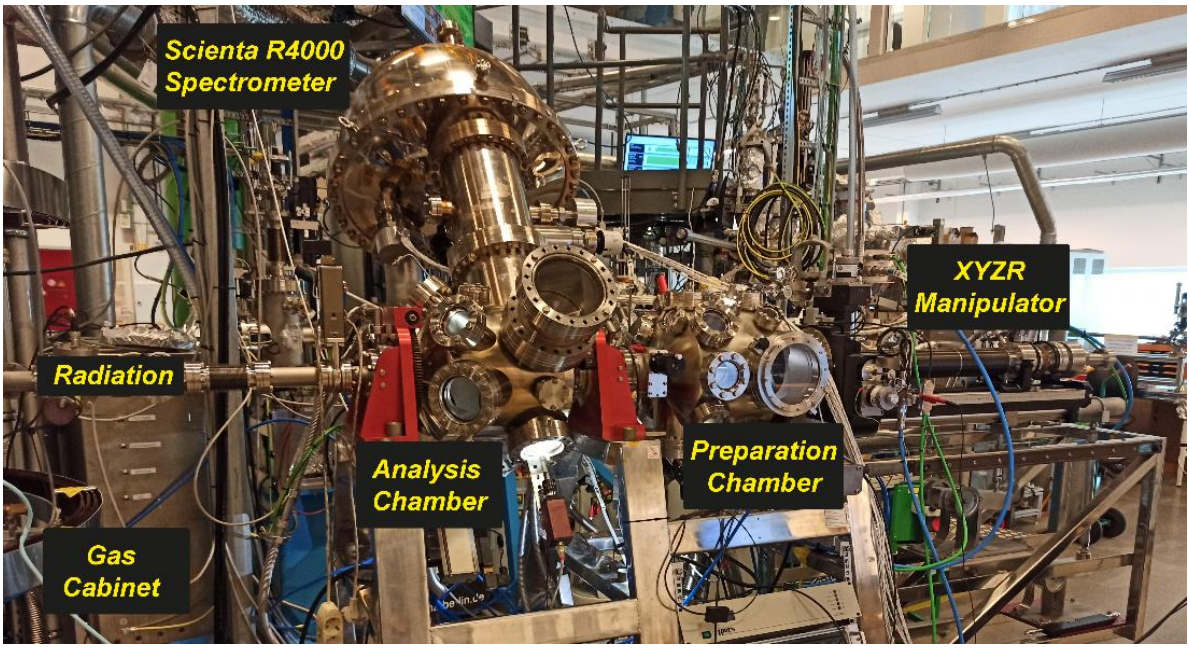

***Figure 2.13**: Layout of the EB02 endstation. The ionization/analysis chamber and the preparation chamber are positioned along the light direction and separated by a manual CF63 valve. Rotation feedthroughs of the analysis chamber are held with the metal supports (in red). The VG Omniax XYZR manipulator to the right is also mounted along the light direction.*

2.3.2 Sample delivery systems

The EB02 end station has been designed for PES experiments on vastly diverse types of samples. Most of these samples are meant to be created in-situ in form of volatile (LDM) targets by dedicated peripheral setups. This modular approach allows us to consider these sample delivery systems as pooled resources and share them on demand with other beamlines, e.g., FinEstBeams. At present, there are four standalone sample delivery systems of this kind:

1. An in-house built flange-mounted gas cell (Figure 2.14) can create a dense gas/vapour environment in a closed compartment with a small entrance hole left for incoming x-rays. Despite a continuous gas/vapour flow through the cell, good vacuum around it is preserved using a home-built differential pumping arrangement. The cell is equipped with facilities for in-situ alignment.

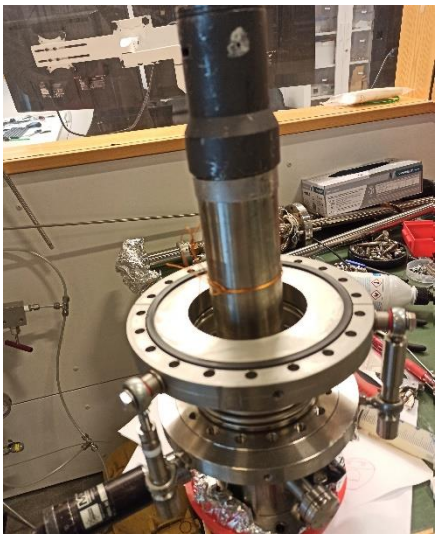

***Figure 2.14**: The in-house built gas-cell with the CF160 flange for mounting on the corresponding port of the Analysis chamber. The differential pumping arrangement ensures that irradiated vacuum compartment can sustain 1 mbar pressure inside it. The upper part (with the graphite-painted cylinder) is placed in the vicinity of the spectrometer lens. The light comes through a hole surrounded by a spot of fluorescent paint used for alignment. The rotation and tilting mechanisms enable cell alignment.*

2. The molecular/cluster beam apparatus (Figure 2.15) can generate dense beams of free clusters from gases and vapours. It is equipped with large turbo-pumps for efficient differential pumping[5]. When attached to a CF160 port of the end station (perpendicular to the light direction), the setup is separated from the analysis chamber via a skimmer with a 0.3-0.5mm pinhole, mounted right in front of the ionization point. To handle the gas load, we further use either an additional turbo-pump installed on the end station opposite to the target beam or a liquid nitrogen cool trap (in the case of clusters produced from liquids).

***Figure 2.15**: Molecular/cluster beam setup with the 50–micron nozzle for gases (not vapours) mounted. The setup is built on a commercial 6-way CF160 cross with two ATH-500 maglev turbo-pumps backed by a corrosive-gas and moisture resistant dry forevacuum pump. The nozzle is mounted at the tip of the rod held by an XYZ VG Omniax 400-mm Z-drive manipulator. The nozzle can be replaced by a heated vessel for producing beams of molecules and clusters out of liquids.*

3. In the liquid-jet setup (Figure 2.16) a thin jet of liquid is made to intersect with the x-ray beam, enabling studies of chemistry of solutions by PES at the scale of individual molecules[6]. The sample is introduced into vacuum using standard HPLC (high-performance liquid chromatography) equipment, and the jet is formed with a cylindrical quartz nozzle (from Advanced Microfluidic Systems GmbH), typically with an opening diameter of 20-25 µm (development of nozzles forming flat sheets are in progress, see section on development). The choice of samples is limited by the vapour pressure of the

[5] M. Tchaplyguine et al., Photoelectron spectroscopy of free clusters. In Handbook of Nanophysics, Ed. K.Sattler, Taylor & Francis, 2011.
[6] N.Ottosson et al., Chem. Phys. Lett. 543, 1 (2012).

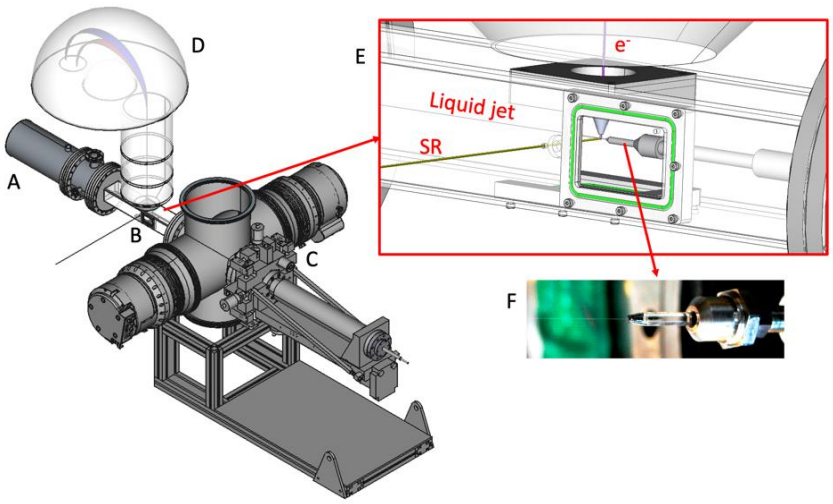

***Figure 2.16**: Sketch of liquid-jet setup at FlexPES. The liquid nitrogen cold trap (A), the differential pumping compartment (B), and the pumping chamber with a manipulator are mounted on the FlexPES EB02 endstation (with spectrometer (D)) during experiments. In insert (E), a detailed view of the nozzle and "skimmer" inside the differentially pumped compartment is shown, and in (F) a photograph of the nozzle and jet.*

solvent (methanol and hexane, with vapour pressures of 130 and 176 mbar @20 °C, respectively, are on the limit in practice), viscosity, and pH (allowed range 1-13). The samples also need to be conductive for PES measurements, which necessitates co-solvation of some ionic compound (at a concentration of a few mM) for non-dissociating molecules. To obtain sufficient signal for conventional core-level PES, bulk-solvated solutes need to have a concentration of tens of mM for aqueous solutions or higher (≈1 permille), but for highly surface-active species concentrations of mM are sufficient. The setup allows controlling the temperature of the sample using a 'jacket' with circulating liquid around the tubing where the sample liquid flows, most frequently used to lower the temperature of the sample to decrease the vapour pressure. The rod for the liquid-jet setup can be electrically insulated to permit biasing the sample, which allows signal from the gas- and the liquid-phase molecules to be separated in kinetic energy (otherwise they often overlap). To handle the substantial vacuum load during operation, the liquid jet is separated from the spectrometer chamber in a differentially pumped compartment (pumped by two high-capacity turbo pumps), with a small opening towards the spectrometer lens at the tip of a conical "skimmer". The liquid is deposited into a liquid nitrogen cooled trap on the opposite side, freezing it immediately after the interaction with the x-rays.

4. The so-called metal-nanoparticle source (Figure 2.17) can produce a beam of nanoscale particles of metals, oxides, nitrides, hydrides, and sulphides from solid targets by magnetron sputtering[7]. It also has dedicated equipment for differential pumping and is separated from the analysis chamber by a skimmer with an opening of 1-2 mm mounted right in front of the ionization point. An additional turbo-pump is usually necessary for keeping the pressure acceptable; it is mounted directly on the analysis chamber below the beam.

[7] M. Tchaplyguine et al., Multicomponent Nanoparticles for Novel Technologies. In 21st Century Nanoscience – A Handbook. Ed. K.Sattler, Taylor & Francis, 2020.

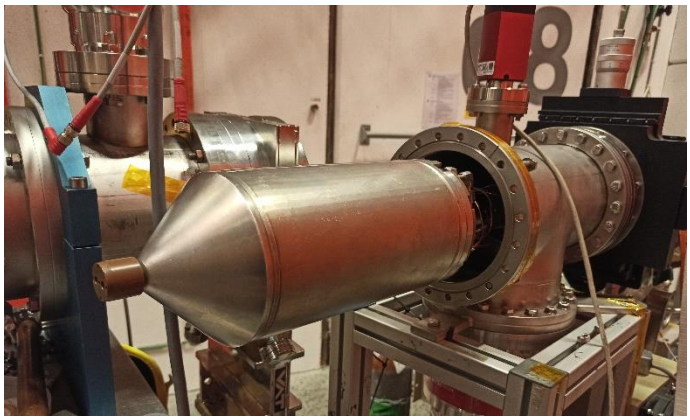

***Figure 2.17**: The nanoparticle source consists of a T-type CF160 chamber with an Omniax XYZ manipulator. A cryostat with a copper cylindrical nozzle (seen in the front) is mounted on the rod of the manipulator. The magnetron sputter gun is placed inside the double-wall cryostat which is cooled with a continuous flow of liquid nitrogen. The source is mounted on the end station's CF160 port perpendicular to the light direction.*

A dedicated differential pumping stage is necessary with each type of the peripheral equipment described above since the Scienta R4000 spectrometer is designed to operate in the range of pressures not worse than a few units in the 10^{-5} mbar range.

In combination with the possibility to introduce and study supported (usually non-UHV) samples using the Preparation Chamber with its manipulator, as well as the Introduction Chamber, the available set of peripheral LDM systems provides remarkably high flexibility in the selection of research objects.

2.4 ICE[8] end station: multi-coincidence momentum imaging on gas phase targets

2.4.1 Overview

The ICE end station (Figure 2.18) is a mobile coincidence spectroscopy end station equipped with a Reaction Microscope (REMI). Reaction microscopes can be used for high resolution measurements of the three dimensional momentum distributions of electrons and ions. With their ability to detect a number of particles in coincidence, they are particularly suitable to the investigation of photo-induced molecular processes / fragmentation dynamics of molecules and clusters.

With no LDM-dedicated beamline at MAX IV, the AMO (atomic, molecular and optical) /LDM community strongly expressed the need for a mobile coincidence spectroscopy end station to enable high resolution coincidence experiments at the lab. ICE was funded by the Swedish Research Council as part of the "Transfer Package" project.

The AMO/LDM user community comprises a field of scientists with expertise in various multi-coincidence techniques and thus a prerequisite for the ICE end station was that it must be adaptable enough to cater to a wide range of research questions. The COLTRIMS reaction microscope from RoentDek GmbH is adjustable in length and electrostatic field geometry - affording some technical flexibility (and therefore a broad scientific applicability). With the possibility to adjust the applied fields, the instrument can also be used during both single bunch and multi-bunch delivery.

[8] Ions in Coincidence with Electrons

2.4.2 ICE infrastructure

The ICE infrastructure is designed to ensure that the setup can be moved with relative ease between beamlines and optimally aligned with the synchrotron beam. This is achieved by ensuring that the footprint of the entire setup is as small as possible. Leg extensions are utilized in order to correct for significant height differences between beamlines, and a "fine adjustment table" enables a high degree of alignment. The material for the vacuum chambers and stand are carefully chosen to ensure as small as possible a distortion of the applied magnetic field (generated by the Helmholtz coils).

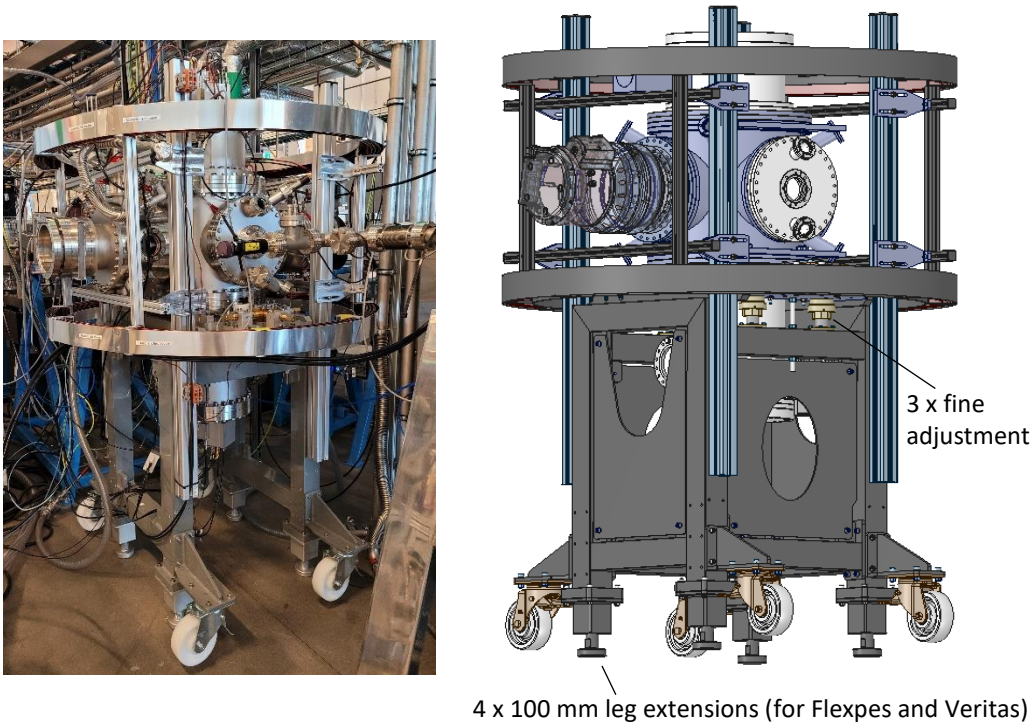

***Figure 2.18**: (left) ICE end station installed at FlexPES beamline, (right) ICE stand – compatible with different beamlines.*

The main vacuum chamber is a multi-port CFEL-ASG multipurpose (CAMP) chamber[9] that is specifically designed for AMO experiments involving imaging/photoexcitation techniques. The vacuum chamber extensions are custom designed to ensure flexibility in their assembly (i.e. they can be repositioned/removed depending on the chosen length of the ion and electron spectrometers) and the strategically-placed windows aid safe mounting of the detectors.

Differential pumping assembly

The ICE detectors cannot operate at pressures above $1e^{-6}$mbar and optimal coincidence conditions (i.e. with low background count rates) require the pressure in the main chamber to be maintained as low as possible during experiments. This is achieved using a multi-stage differential pumping arrangement (Figure 2.19) such that even with a pressure of e^{-2}mbar in the source chamber, the pressure in the main experimental chamber is on the order of e^{-7}/e^{-8}mbar. The differential pumping arrangement comprises two beam skimmers mounted in separate differential stages that are pumped by separate sets of turbo pumps.

[9] Strueder et al., Nucl. Inst. Meth. Phys. Res. A, 614 (2010) 483.

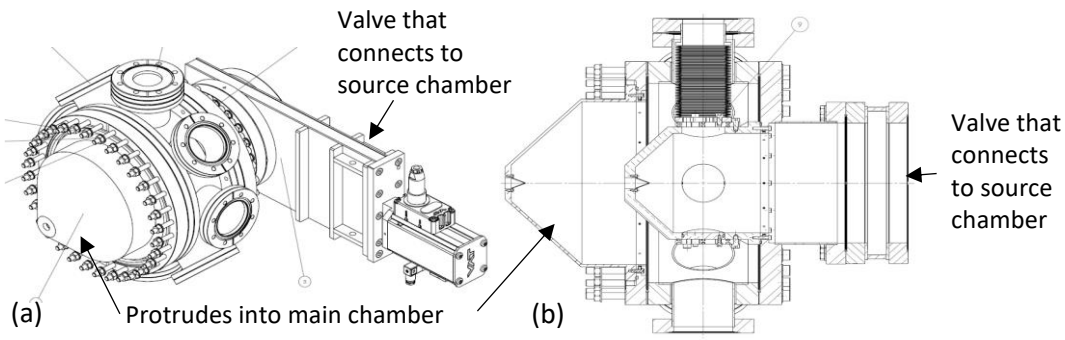

***Figure 2.19**: Differential pumping arrangement (a) 3D drawing of differential pumping arrangement (b) 2D drawing of the different pumping stages. The molecular/cluster beam setup is connected to the valve indicated in the figure.*

2.4.3 Reaction microscope

The REMI is comprised of two time-of-flight (ToF) spectrometers (electron and ion) mounted opposite to each other on opposite sides of an *"interaction region"*. The spectrometer consists of a number of open copper electrodes (mounted 5 mm apart), which can be connected in various ways in order to realise different electrostatic field configurations (Figure 2.20). Further components, for example, fine meshes, lens electrodes of varying diameter etc. are also available for use in future configurations of the spectrometer system.

***Figure 2.20**: (a) The ICE REMI – composed of a number of copper electrodes stacked 5mm apart. It is possible to adjust the length and electrostatic field geometry of the instrument. (b) The mounted spectrometer. The interaction region is aligned with the second skimmer of the differential pumping arrangement. (c) Copper electrodes connected via 1MΩ resistors.*

In the present design, all but two electrodes in each spectrometer are connected to each other *in vacuo* via 1MΩ resistors (photo in Figure 2.20 and schematic in Figure 2.21). The electrodes that are not connected *in vacuo* are connected outside of vacuum and feedthroughs are used to apply voltages to specific electrodes. With this arrangement it is possible to interchange between two different operational modes without breaking vacuum. The *COLTRIMS mode* typically employs lower electric

fields with all of the copper electrodes connected in series via 1MΩ resistors. In that mode, a magnetic field is also applied via Helmholtz coils (to ensure that high energy electrons will not be lost from the spectrometer before reaching the detector). The *High-field Lens mode* can be achieved by replacing the external 1MΩ connection(s) in either/both of the ion and electron spectrometers with voltage dividers and power supplies. The flexible design - utilizing external connections for the few relevant electrodes - ensures speedy interchange (~5-10 min) between the above two described operational modes. The ability to switch between these two modes without breaking vacuum is especially crucial given that the *COLTRIMS mode* can only be used during single bunch delivery when the time between photon pulses is sufficiently long (320 ns in the case of MAX IV). In multi-bunch delivery, the temporal gap between photon pulses is much shorter (10 ns) and hence higher potentials and a lens arrangement are required (without a B field) to ensure that the electron ToF's are sufficiently short (~

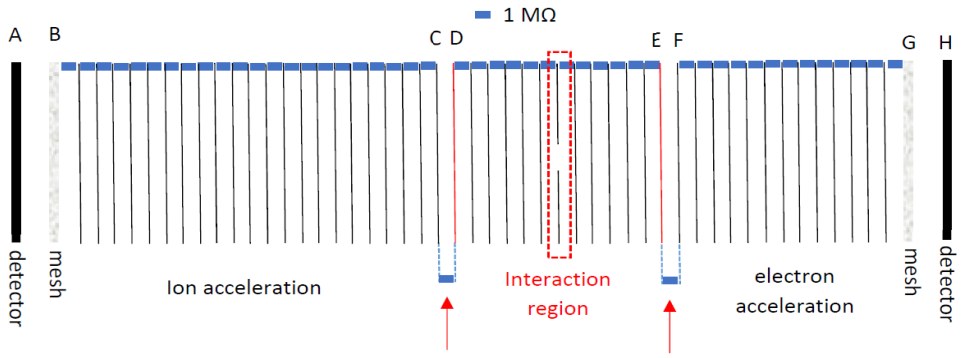

***Figure 2.21**: ICE spectrometer connections – red arrows indicate that external connections are used to enable interchange between two different operational modes. External feedthrough connections indicated by letters. The configuration indicated in the above schematic shows the COLTRIMS mode. (Note: This figure is representative and does not indicate the entire number of electrodes used in the spectrometer.)*

2-7) ns.

2.4.4 Detectors, Front-end electronics and Data acquisition

The REMI is equipped with two RoentDek HEX100-75 delay line/MCP detector arrangements (Figure 2.22), i.e. 3-layer delay line detectors (diameter: 100 mm) and MCP's of 75mm diameter (MCP's of 100 mm diameter can also be mounted). Position encoding is achieved by measuring the signal arrival time difference at both ends of each parallel-pair delay line. Whilst only two delay line wires are required to calculate the 2D position of a particle, the additional delay line layer used in the Hexanode detector ensures optimal signal collection and improved multi-hit performance.

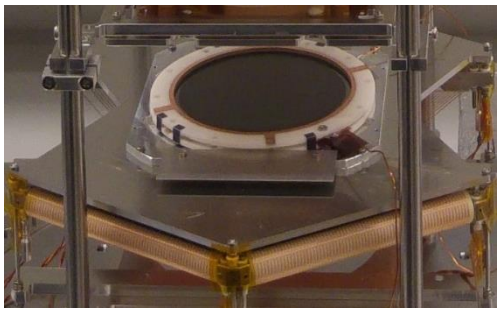

***Figure 2.22**: RoentDek HEX 100-75 detector configuration. The HEX detector has 3 layers of wires offering enhanced detection efficiency compared to the two-layer DLD version. Principle of operation: The time difference between the two signal pulses at the end of each delay line wire is proportional to the hit position on the detector.*

Signal decoupling plugs provided by the manufacturer are used to convert the signals from the differential delay-line pairs into single-line signals. Seven signals are produced for each impacting particle and electronic readout/processing of these signals is achieved using fast timing amplifiers and

fADC digitizers. The fADC units sample the complete signal trace from the detectors. Used in conjunction with the CoboldPC software, it is possible to analyse the shape of the signals and perform a calibration of the hexanode detector.

2.4.5 Capabilities developed in-house

Data analysis and Universal data format

The standard data format (available with RoentDek's CoboldPC data acquisition (DAq) and analysis (DAn) program) is list mode data where all acquired information is stored event by event in a list mode file (lmf). During measurements, the data is processed and depicted in various plots defined by the DAn. The list mode data can also be processed offline using the DAn and/or the CoboldPC source code, offering the possibility of *"replaying the experiment"*, applying various corrections to improve data quality or performing in-depth data analysis. However, the CoboldPC source code is written in C++ and many user groups have their own data analysis programs that are incompatible with lmf data format.

In order to improve data accessibility, an in-house project with the MAX IV KITS software group was executed to ensure the possibility of converting the lmf data to HDF5(xyt) – ideally after the hexanode has been calibrated.

Ion yield measurements using photon energy scanning

The ICE detectors have been incorporated into the FlexPES TANGO control and MAX IV Sardana control systems in order to provide the capability of recording Total Ion Yields as a function of photon energy. Figure 2.23 (a) and (b) provide examples of ion yield spectra recorded with ICE at FlexPES. The two data sets were calibrated using Ederer1975 and Sodhi1984, respectively[10].

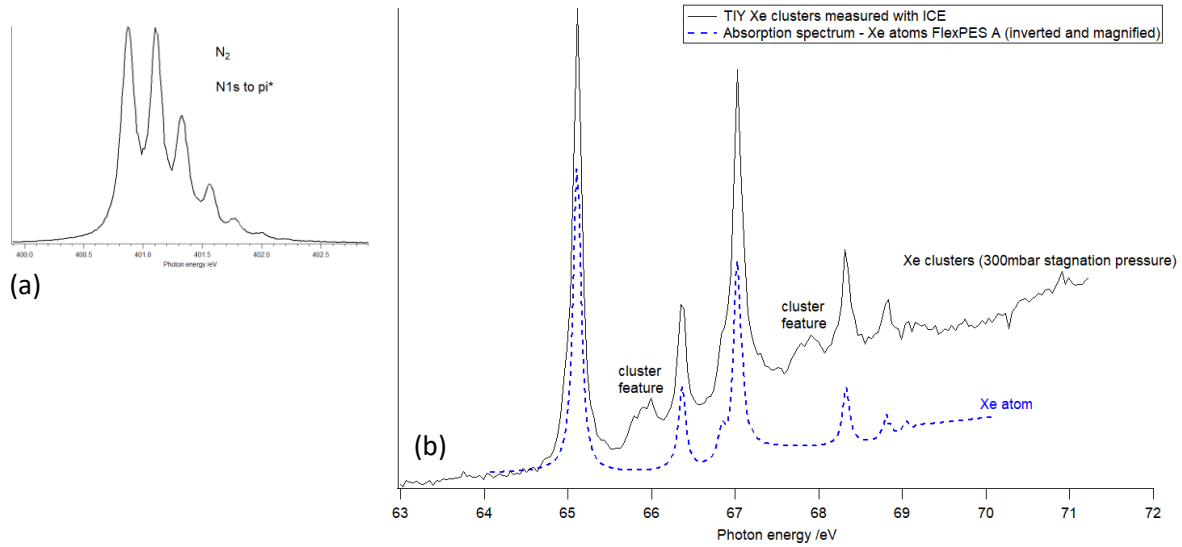

***Figure 2.23**: Total Ion Yield Spectra: (a) Total Ion Yield of Molecular N_2 at the Nitrogen edge (b) Total ion yield recorded for Xe clusters using ICE and absorption spectrum recorded for Xenon atoms at FlexPES. The cluster features can be distinguished from the atomic features.*

2.4.6 ICE detection capabilities

Each operational mode of ICE has different detection capabilities (that are dependent on the design and geometry of the spectrometer). For the current setup, the following capabilities are valid:

COLTRIMS mode

[10] Ederer, J. Optical Soc. Am., 65 (1975) 634. Sodhi, J. El. Spec. Rel. Ph., 34 (1984) 363.

- Max. Kinetic Energy detected (electrons): 60 eV (tbc). Note: it should be possible to detect up to 100 eV electrons with an electron spectrometer of different geometry.
- Max. KE detected (ions): 10 eV

High Field Lens mode

- Max. Kinetic Energy detected (electrons): 15 eV
- Max. Kinetic Energy detected (ions): 10 eV

2.4.7 Compatible sample delivery systems

The ICE end station can be used with the molecular/cluster beam apparatus (described in Section 2.3.2). With that sample delivery system, it is possible to generate dense beams of atoms, molecules or free clusters from gases and vapours. By varying the nozzle size and stagnation pressure in the source it is possible to vary the source conditions and even the size range of clusters produced.

3 Beamline operation

3.1 Modes of operation and statistics overview

FlexPES received first light for commissioning in June 2019 and has been open for regular user proposals since spring 2020. According to MAX IV policy, 75% of beamtime should be made available to general users through a peer-reviewed proposal system. The remaining 25 % can be used for maintenance, commissioning, and in-house research.

Standard access. Beamtimes at FlexPES are normally allocated in 30 4h-shift blocks (5 24-h days, Wednesday-Sunday). Mondays are reserved for accelerator needs, and Tuesdays are dedicated to beamline and insertion device commissioning and maintenance. (Soon this may change, with Tuesdays going into the standard user operation too.) On a few occasions, shorter allocation blocks have been used, e.g. 12 and 18 shifts in one week, allowing two proposals to go ahead in the same week. This practice will probably become more common in the future, in order to accommodate more proposals and use the time more efficiently.

Due to the COVID-19 pandemic some deviations from regular operation have occurred. Travel limitations have been in place between June 2020 and September 2021, and for a large part of spring 2021 activities ceased completely during a period of lock-down. The beamline still has, except for the lock-down period, largely been in operation, partially in **remote access** mode with no external users present. The remote access mode was enabled with all necessary control software available to the external groups remotely on a dedicated server. Three one-week beamtimes were carried out in this mode in the spring 2021.

Fast access. Apart from “normal” proposals, from March 2023 we offer an opportunity to apply for the fast access (FA). The FA proposals are foreseen for testing the sample or approach feasibility; they should help (especially new users) in preparation of the normal proposals for a later call. The FA at FlexPES is limited at the moment to maximum 2 shifts (8 hours) of beamtime per proposal.

Training & Education access. FlexPES has also been used for teaching: In the course *Introduction to synchrotron-radiation based science* at Lund University, a lab has been arranged every autumn since 2019, informally 2019 and 2020, and within the new Teaching and Education proposal cycle in 2021. Two proposals have been accepted for the autumn 2022 term, 6 shifts for the course *Introduction to*

synchrotron-radiation based science and 2 shifts for the course *Spectroscopy and the quantum description of matter*.

3.1.1 Proposal statistics

In Table 3, the statistics regarding submitted and accepted proposals from VT2020, when the first general call for FlexPES was opened, until fall 2022 (scheduled but not yet performed beamtime) are summarized. The division of accepted proposals between branch A and B primarily reflects the ratio of submitted proposals for the two branches.

Table 3: History of submitted and accepted proposals.

	VT20	HT20	M VT/HT21	VT22	HT22
Submitted	26	33	43	33	35
Accepted A/B	6/4	15/2	9/5	10[1]/4	7/5[2]
Oversubscription	2.6	1.74	3.31	2.36	2.92

[1] 2 proposals shared 1 week, 13 weeks scheduled in total

[2] Preliminary numbers, proposals on waiting list may be accepted

In Table 4, the scheduling of beamtimes from autumn 2019, when the first external users were invited as commissioning experts, until fall 2022 are summarized. Note that the period HT lasts from September-February and VT from March-July. With the limitations on travel and lab access during the COVID-19 pandemic, proposals accepted in the periods VT20 until M(erged) VT/HT21 have in several cases been postponed and scheduled in a later period.

Table 4: Division of beamtime at FlexPES (in weeks)

	HT19[1]	VT20	HT20[2]	M VT/HT21[2]	VT22	HT22
Expert comm.	4	0	0	1	0	0
In-house	3	6	0	1	2	0
General	0	7	12	21	13	12[3]
BL comm.	13	4	2	3.5	0	2.5
Total	20	17	21	34.5	15	18.5
General share	0%	41%	57%	61%	87%	65%

[1] No open call, only invited experts

[2] Lab closed for users due to COVID 19 Jan – May 2021

[3] Preliminary number, proposals on waiting list may be accepted

Of the accepted normal proposals, approximately half have been from Swedish users (affiliation of main proposer), a tenth from Nordic and Baltic countries, a third from EU and associated countries, and a twentieth from the rest of the world. There are no quotas for local users, the allocation is entirely based on the peer-review evaluation by the Program Advisory Committee (PAC).

3.1.2 User feedback

The MAX IV Laboratory solicits feedback from all users after each beamtime, regarding their satisfaction with the operation and performance of the beamline and other services. The feedback has generally been very positive, as can be seen in Figure 3.1, where the average scores for some key parameters are shown. User experimental reports and feedback forms are very helpful in identifying and fixing any beamline related concerns, and are often an inspiration for further developments.

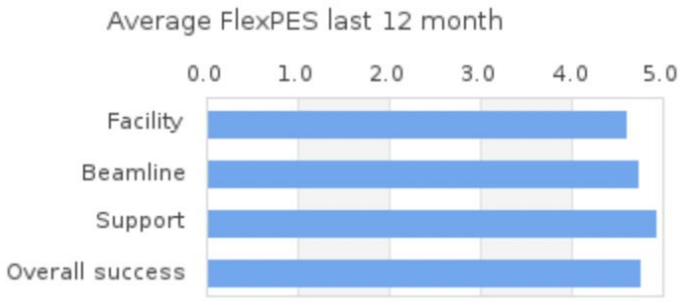

***Figure 3.1**: Average user feedback scores for the last 12 months (as of July 11, 2022).*

3.1.3 Publications

As of this writing (September 2022), 17 papers have been published in peer-reviewed journals, which have (fully or partially) been based on work at FlexPES; 1 in 2020, 11 in 2021, and 6 in 2022. Many more papers are known to be either in preparation or submitted.

FlexPES publication list:

1. Robin Athle et al., *Improved Endurance of Ferroelectric HfxZr1–xO2 Integrated on InAs Using Millisecond Annealing*, Adv. Mater. Interfaces, 2201038 (2022)
2. Jaanus Kruusma et al., *The electrochemical behaviour of butyltrimethylammonium bis(trifluoromethylsulfonyl)imide at negatively polarised aluminium electrode studied by in situ soft X-ray photoelectron spectroscopy, electrochemical impedance spectroscopy and cyclic voltammetry techniques*. J Solid State Electrochem, in press (2022).
3. Alberto Garcia-Fernandez et al., *Experimental and Theoretical Core Level and Valence Band Analysis of Clean Perovskite Single Crystal Surfaces*, Small 2106450 (2022)
4. Yen-Po Liu et al., *Hydrogen plasma enhanced oxide removal on GaSb planar and nanowire surfaces*, Applied Surface Science **593**, 153336 (2022)
5. C. J. Weststrate and J. W. Niemantsverdriet, *CO adsorption on Co(0001) revisited: High-coverage CO superstructures on the close-packed surface of cobalt*, Journal of Catalysis **408**,142-154 (2022)
6. Abdul Rahman Abid et al., *The effect of relative humidity on CaCl2 nanoparticles studied by soft x-ray absorption spectroscopy*, RSC Advances **11**, 2103-2111 (2021)
7. Stephan Appelfeller, *Investigation of single-domain Au silicide nanowires on Si(110) formed for Au coverages in the monolayer regime*, Scientific Reports **11**, 14771 (2021)
8. Robin Athle et al., *Effects of TiN Top Electrode Texturing on Ferroelectricity in Hf1-xZrxO2*, ACS Applied Materials & Interfaces **13**, 11089-11095 (2021)
9. Yongzhen Chen et al., *Understanding Interface Dipoles at an Electron Transport Material/Electrode Modifier for Organic Electronics*, ACS Applied Materials & Interfaces **13**, 47218-77225 (2021)
10. Johannes Kirschner et al., *The molecular structure of the surface of water-ethanol mixtures*, Physical Chemistry and Chemical Physics **23**, 11568-11578 (2021)
11. Alfred Larsson et al., *Thickness and composition of native oxides and near-surface regions of Ni superalloys*, Journal of Alloys and Compounds **895**, 162657 (2022)
12. Alexei B. Preobrajenski et al., *Honeycomb Boron on Al(111): From the Concept of Borophene to the Two-Dimensional Boride*, ACS Nano **15**, 15153 (2021)

13. Mamidala Saketh Ram et al., *High-density logic-in-memory devices using vertical indium arsenide nanowires on silicon*, Nature Electronics **4**, 914-920 (2021)
14. Cody M. Sterling et al., *Sensitivity of Nitrogen K-Edge x-ray Absorption to Halide Substitution and Thermal Fluctuations in Methylammonium Lead-Halide Perovskites*, Journal of Physical Chemistry C **125**, 8360-8368 (2021)
15. Robert Temperton et al., *A soft x-ray probe of a titania photoelectrode sensitized with a triphenylamine dye*, Journal of Chemical Physics **154**, 234707 (2021)
16. Chi-Yuan Yang et al., *A high-conductivity n-type polymeric ink for printed electronics*, Nature Communications **12**, 2354 (2021)
17. Marcel J. S. Abb et al., *Thermal Stability of Single-Crystalline IrO2(110) Layers: Spectroscopic and Adsorption Studies*, Journal of Physical Chemistry C **124**, 15324-15336 (2020)

3.2 Staffing

The FlexPES team consists at present of three permanently employed beamline scientists, one research engineer, a half of the beamline technician (position shared with the SPECIES beamline) and one temporary employed postdoc (the number of postdocs can vary). In addition the team is supported by the work of the MAX IV LDM coordinator (Noelle Walsh) who is formally not a part of the FlexPES staff but is responsible for the ICE end station. All of the scientists were running various soft x-ray beamlines at the MAX II ring (I1011, I411 and D1011) prior to its shutdown in 2015. They (along with the research engineer, Alexander Generalov) were also responsible for planning and delivering the FlexPES beamline project.

Alexei Preobrajenski (Beamline manager and scientist, permanent) Overall responsibility for the beamline operation and development, specific focus on the SMS branch. Participates in user support and local contact duties.

Maxim Tchaplyguine (Beamline scientist, permanent) Responsibility for the LDM branch and EB02 end station. Participates in user support and local contact duties.

Gunnar Öhrwall (Beamline scientist, permanent) Responsibility for the liquid jet setups and development and the chopper project. Participates in user support and local contact duties.

Alexander Generalov (Research engineer, permanent) Responsibility for the technical developments with focus on software development. Participates in user support and local contact duties.

Noelle Walsh (MAX IV LDM activity coordinator, permanent) Role at FlexPES: responsibility for the ICE station project.

Stephan Appelfeller (50% duties as a beamline technician, permanent) Technical assistance in installations and preparation for experiments. Employed from August 2022. Worked as a postdoc at FlexPES in 2019-2022.

Eleanor Frampton (postdoc, temporary) Started in September 2022; pursuing an independent research project on covalent molecular networks. May participate in user support in the future.

Of great help for the smooth operation and development at FlexPES are also the beamline contacts in the specific infrastructural support teams, especially IT software (Anton Joubert) and IT hardware (Suleyman Malki).

3.3 Typical beamtime process

Beamtime allocation. Similar to other MAX IV beamlines, there are two rounds of proposal calls at FlexPES annually. At first, all submitted proposals are a subject of pre-screening by the BL staff for feasibility. Once this check is passed, all proposals are evaluated by the specific Program Advisory Committees (PAC). In our case there are two PACs: one for the SMS experiments, and one for the LDM projects. Each PAC provides a ranking of the submitted proposals, so that those on the top of the list have higher chances of being accepted. As two different PACs can have different absolute ranking standards, we use quotas for each branch to ensure more homogeneous distribution of beamtime for the two different user communities. The specific quota for each branch is an average of two factors: the number of research proposals submitted to it, and the number of different research groups behind the submitted proposals (the latter is to discourage multiple submissions from one single group). For example, in the last call the beamtime share of the SMS (LDM) branch was ca. 57% (43%). The amount of time to be allocated for each proposal is requested by the respective user but can be reduced by the PAC if deemed reasonable. Normally we allocate 5 full days per proposal, but also have had 2- and 3-days sessions. With possible introduction of 6 beamtime days per week (as planned by the management), this practice can change.

Beamtime scheduling. The scheduling of accepted projects is performed in coordination with the PIs of the respective groups. Normally all of them are contacted by the BL staff at least two months before the first experiment has to begin with a request to provide most and least convenient time slots for their experiments. Once the schedule converged to everybody's satisfaction, it is placed into the DUO system and all PIs receive an official notification and further instructions.

Preparation for beamtime. A local contact (LC) from the BL team is assigned to each accepted project in good time. The LC is responsible for communication with the respective PI before the arrival of the scheduled research group on the following matters:

- questions on experimental setup, specific preparations needed, availability and status of any relevant equipment
- advice in any practicalities (although this is more a responsibility of the User Office)
- safety issues and contact with the MAX IV Experimental Safety Team (EST)
- follow-up on the necessary measures, like whether or not the users have created Experimental session, declared their samples and submitted the Risk Assessment forms.

Support during beamtime. The LC is meeting with the respective group upon their arrival (preferably a day before the beamtime starts). He/she

- shows them the premises, the experimental station, all relevant equipment and laboratories
- explains how the end station works
- discuss the details of sample mounting, extra equipment installation and experimental schedule
- assists (together with other staff members) in sample mounting, installation of user's equipment, pumping, bake-out, etc
- (once the beam is available) shows how to operate the end station and the beamline, both hardware- and software-wise.
- Assists in selecting optimal measurement parameters
- Helps to resolve all issues related to the experiment (involving other staff members if necessary) by providing a continuous support channel during working hours.

As a rule, the LC also provides the on-call support till 23:00 on weekdays and from 8:00 to 20:00 on Saturday and Sunday. Often a dedicated group is created in a messenger (e.g. WhatsApp) to facilitate the information flow between the external researchers and the supporting staff. The staff is also assisting the user groups with preliminary data analysis/representation (if necessary), by providing a set of dedicated in-house procedures for Jupiter Notebook and Igor Pro. In the future we plan to further improve support in preliminary data treatment, as it helps the users to make right decisions in their workflow faster and more efficiently.

To improve the user experience and efficiency, and to reduce the load on the staff to a sustainable level, considerable efforts are put by the FlexPES team to automate experiments, simplify graphical user interfaces, improve software stability, introduce various machine-protecting interlocks and safety features, and to maintain detailed instructions on all aspects of experimental operation via internal Wiki pages.

3.4 Community outreach

To attract users and to be relevant for the user community, it is of paramount importance to reach out to current and potential users, and we actively try to do this through several channels.

Basic outreach

In the normal research activities, there are many channels where knowledge about the beamline is disseminated, for instance:

- FlexPES web pages (updated August 2022 along with the general MAX IV web site update) containing all relevant information on the capabilities and status of the equipment at the BL and all end stations.
- LDM web pages providing specific information on the equipment relevant to AMO research at a number of beamlines, including FlexPES.
- Fast Access mode of operation (offered to the community from the autumn 2022 call): many more groups will be able to try some measurements as a feasibility check, with the potential consequence of attracting them as new regular users.
- User publications and conference presentations of work done at the beamline, or word-of-mouth in research community.
- Dedicated lectures about FlexPES and other MAX IV photoemission beamlines given by the staff e.g. at Chalmers and Uppsala Universities (twice in each) and Luleå University (once).
- MAX IV outreach activities where the beamline staff contribute, such as presentations at MAX IV Scientifika and Science and R&D seminar series; the MAX IV user meeting, including beamline presentations and posters and scientific subsections, e.g. the LDM subsession at the user meeting 2021; aimed news letters to certain categories of users and other interested parties about status and progress at the beamline.
- Organization of international workshops, such as the Next Generation LDM workshop at MAX IV in March 2017 (organized by Noelle Walsh).
- Beamline paper is in preparation.

Outreach through collaborations

Research and development projects with outside groups are natural parts of the attempt to increase the attractiveness of the beamline, while also deepening the connection to the user groups involved in the projects. Such projects are common, and some current examples include:

- Development of Flat jet nozzles for soft x-ray spectroscopy together with the Sample Environment & Characterization group at XFEL (Gunnar Öhrwall and Noelle Walsh).
- The Trapped Ion Spectrometer Setup (TRISS) for MAX IV beamlines, collaboration with researchers at the Department of Physics, Uppsala University but supported by several other institutes (Noelle Walsh).
- External postdoc projects, e.g. development methods for in-operando electrical measurements in collaboration with LTH (Lunds Tekniska Högskola), run by a former postdoc Andrea Troian.
- Postdoc research projects involving their former group members, e.g., a project of Stephan Appelfeller on the silicide nanowires in collaboration with TU Berlin, or a project of Eleanor Frampton on the covalent molecular architectures in collaboration with Nottingham University.

Outreach through educational efforts

Training the next generation of scientists and engineers is one of the fundamental objectives of MAX IV, and the staff at FlexPES contribute to this effort in several ways:

- Courses at MSc level: The course *Introduction to synchrotron radiation based science* given at the Department of Physics at Lund University has been organized by Gunnar Öhrwall since 2017, with a lab at FlexPES (since 2019); a lab at FlexPES within the course *Spectroscopy and the quantum description of mattter*, also given at the Department of Physics at Lund University, where Maxim Tchaplyguine and Gunnar Öhrwall contribute with lectures about their research fields, will be arranged in spring 2023.
- MSc and PhD theses based on work at the beamline: Emmanouil Tzomos MSc (title: *x-ray Photoelectron Spectroscopy on Clusters: From Water Clusters to Metal & Metal-Oxide Nanoparticles***,** supervisor Maxim Tchaplyguine, finished January 2021); Tamires Gallo PhD (supervisors Gunnar Öhrwall and Noelle Walsh, preliminary finish date June 2023). The PhD student PRISMAS network project centred at MAX IV was recently approved within the EU Horizon MSCA Cofund program, and while the level of funding is yet to be decided, we hope it will provide opportunities for more PhD students at FlexPES, since several of the scientists at FlexPES (Alexei Preobrajenski, Noelle Walsh, Gunnar Öhrwall) were involved in the application.

4 User and in-house research

Thanks to a very diverse user community at FlexPES, the distribution of the relevant areas of science here is very broad. By September 2022, 54 beamtimes granted by PAC were finished at the beamline (see Appendix III for a complete list of all accomplished projects). They fall into several major categories (number of proposals in brackets): **catalysis** (13), **solar cells** (9), **aerosols** (for climate and other research) (8), **heterojunctions for electronics** (6), **novel 2D materials** (5), **sensor materials** (4), **batteries** (2), **corrosion** (2), **electrochemistry** (2), and more exotic for our methods **palaeontology**, **medicine** and **industrial processing** (one of each). This separation is obviously approximate, as many projects are interdisciplinary and can cover several research areas and potential applications. Below we present a few examples of experimental work performed recently and typical for the core expertise of the beamline.

Spectroscopic studies of on-surface synthesis of chiral graphene nanoribbons on Au(788) I. I. Chunin, L. E. Gannon, A. A. Cafolla, V. De Renzi, N. Cavani, A. Nefedov, Z. Chen, A. Narita, K. Muellen and C. McGuinness, *manuscript in preparation*.

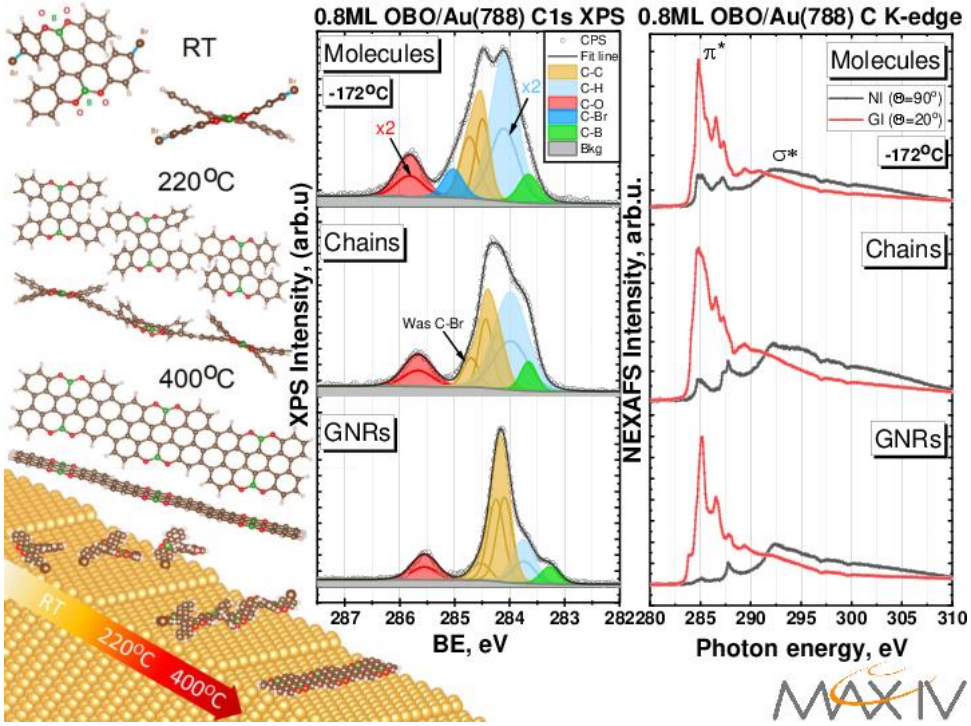

***Figure 4.1**: The on-surface synthesis of OBO-nanoribbons. Left: stages of synthesis shown schematically. Right: XPS and NEXAFS spectra corresponding to the main stages: free precursor molecules, molecular chains and nanoribbons.*

Engineering of graphene nanoribbons (GNRs) with different structure and functionalities opens up new routes in electronics, sensors and catalysis. Here, the on-surface synthesis of the *6,16-dibromo-9,10,19,20-tetraoxa-9a,19a-diboratetra-benzo[a,f,j,o]perylene* graphene nanoribbons (OBO-GNRs) which embed O-B-O motifs along the zigzag edges in this heteroatom-doped chiral (4,1)-GNR[11] was examined by high resolution core level XPS and NEXAFS spectroscopy on vicinal stepped Au(788) surface. Shown in Figure 4.1 from top to bottom are the stages of deposition of the molecules, annealing to 220^{O}C sufficient for debromination and Ullmann coupling and a chain formation to have completely occurred (monitored by Br 3d XPS not shown), and then further annealed to 400^{O}C to trigger internal cyclodehydrogenation and the formation of the flat OBO-GNR. At each stage the panels show from left to right the (i) molecular structure, (ii) the high-resolution C 1s XPS and (iii) the C K-edge NEXAFS spectra taken at the normal incidence (NI, shown in black) and grazing incidence (GI, shown in red), separately probing the π* and σ* states. The C K-edge NEXAFS shows a transition from the 'twisted' as-deposited molecules to the flattened chiral (4,1)-OBO-GNR structure. Indeed, the NI spectrum along the (111) terrace normal illustrates a small feature at 285 eV and this is related to the in-plane C-B σ* bond and lower energy empty B 2p components, but otherwise indicates the GNR is parallel to the surface. The peak-fit analysis of the C 1s XPS components (in combination with DFT calculations of core level binding energies) enables us to explain all transformations in detail (e.g., the debromination, where the C-Br bonds turn into strained C-C bonds between formula units, and the gradual change of the C-H components ultimately showing the cyclodehydrogenation reaction).

[11] Wang, X.-Y. et al., J. Am. Chem. Soc. 140, 9104 (2018).

Critical Step in the HCl Oxidation Reaction over Single-Crystalline CeO_{2-x}(111): Oxygen-Induced Site Change of Surface Chlorine V. Koller, A. Spriewald-Luciano, S.M. Gericke, A. Larsson, C. Sack, E. Lundgren, and H. Over, *manuscript in preparation*.

Cerium dioxide has shown to be an active and stable catalyst in the Deacon reaction (4 HCl + O_2 → 2 Cl_2 + 2 H_2O). However, the elementary steps in the reaction mechanism still remain elusive. Here, we investigate the reoxidation of a reduced, chlorinated CeO_{2-x}(111)/Ru(0001) thin film by molecular oxygen. This is a key step in the catalytic reaction as the active catalyst phase is known to be chlorinated. We can show the transition of surface chlorine, initially located in a surface oxygen vacancy, Cl_{vac} to a cerium on-top Cl_{top} position, in accordance with DFT calculations by Amrute et al. in the literature.

Most importantly, we can show via the complementary surface- and bulk-sensitive techniques at FlexPES that first the bulk is reoxidized, and only upon saturation reoxidation and the transition of the Cl-species at the surface takes place. As a bulk-sensitive technique we utilized NEXAFS in total electron yield TEY mode (cf. Figure 4.2, a). For surface-sensitive measurements we used high-resolution XPS (cf. Figure 4.2, b) and resonant photoelectron spectroscopy RESPES (cf. Figure 4.2, c). After reoxidation of the bulk, an abrupt reoxidation is observed at the surface (cf. Figure 4.2, d), accompanied by a shift of the Cl-surface species (cf. Figure 4.2, e).

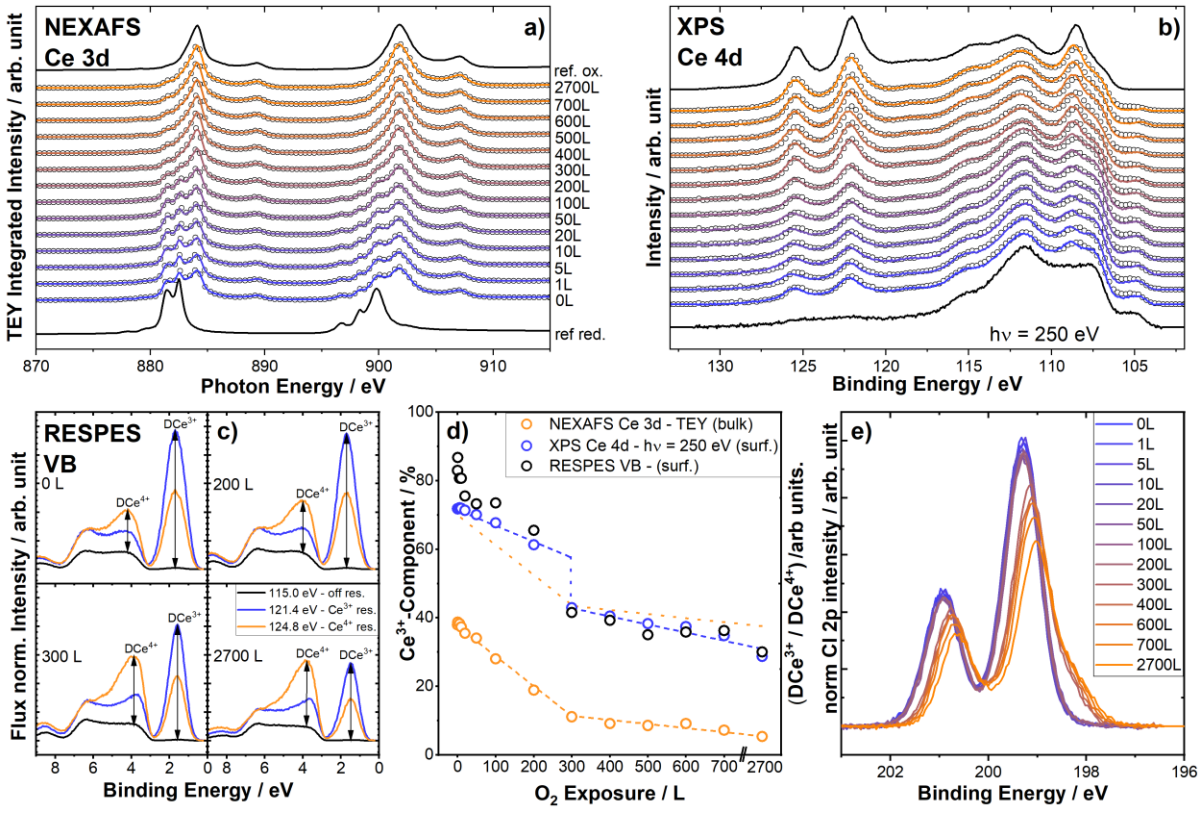

***Figure 4.2**: Depth probing of CeO2_x(111) upon reoxidation with O2. a) Ce 3d NEXAFS b) Ce 4d XPS hv = 250 eV c) RESPES Ce4+-res. hv = 124.8 eV, Ce3+-res. hv = 121.4 eV, off-res. hv = 115.0 eV d) comparison of the oxidation degree at bulk- and surface-level e) Cl 2p XPS hv = 250 eV*

Using ICD to investigate micro-solvation of metal ions – Denis Ceolin (Soleil), *proposal 20211004*

Inter-atomic or inter-molecular Coulombic decay (ICD) is an electronic decay process of inner valence or core holes that involves orbitals centered on neighboring atoms or molecules in weakly bound systems. ICD has been observed in several van der Waals or hydrogen bonded systems[12], and the probability of such decays drops very quickly with distance (an r^{-6} dependence is expected), meaning only nearest neighbors contribute significantly. This property provides an avenue for investigating the immediate surrounding of e.g. a solvated metal ion, and in this project the micro-solvation of Ca^{2+} ions was investigated in two different solvents and for two different counter ions at different concentrations by observing the ICD after 2p ionization, using the liquid micro-jet setup at FlexPES. When changing the molar fraction of ethanol in ethanol-water mixtures from 0 (pure water) to ≈1 (pure ethanol), clear changes in the ICD structures in the decay spectrum from the 2p holes can be observed (see Figure 4.3), with a progression observed for intermediate molar fractions. However, due to the complex final state structure of the decay process, the interpretation is not trivial, and will likely require involvement of state-of-the art electronic state calculations from external collaborators. Changing the counter ion from nitrate to chloride induces some subtle changes in the ICD spectrum (see Figure 4.3), indicating some influence on the immediate solvation shell of the Ca^{2+} ions, most likely due to ion-pair formation in either or both cases. We also observe some influence of solute concentration. The experiments were performed in April 2022 and analysis of the experimental data is in progress. Work on the theoretical calculations needed for a full understanding have yet to be started, and with the complexity of the calculations in mind we can realistically hope to publish during 2023.

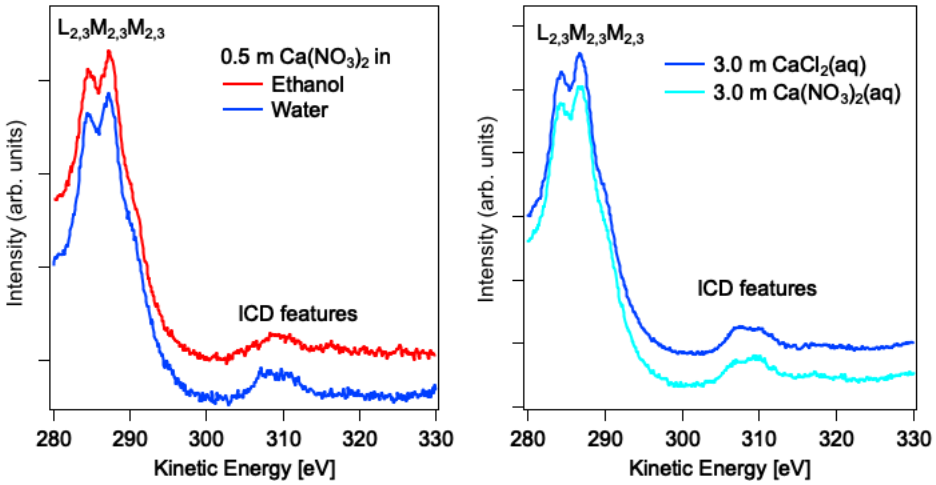

Figure 4.3*: Left: Spectra for 0.5 m $Ca(NO_3)_2$ in water and ethanol in the vicinity of the $L_{2,3}M_{2,3}M_{2,3}$ Auger and $L_{2,3}M_{2,3}V$ ICD features. The spectra have been normalized and shifted in energy to overlap approximately. While the local Auger features are very similar, the ICD features differ in appearance. Right: Spectra in the same range for aqueous solutions of 3.0 m $Ca(NO_3)_2$ and 3.0 m $CaCl_2$, where slight differences in the ICD features can be observed.*

[12] T. Jahnke et al., Chem. Rev. 120, 11295 (2020).

Nanodosimetry: Energy deposition and formation of low-energy electrons in water nanodroplets, - O.Björneholm et al (Uppsala University), *proposal 20190783*

The goal was to study how the primary photon radiation translates into the secondary radiation environment dominated by low-energy electrons in an aqueous environment on a nanometer scale. The primary photon radiation gives through interaction processes rise to a spectrum of secondary particles dominated by secondary electrons. Stepwise ionization via inelastic scattering shifts the electron kinetic energy distribution towards lower energy. It is these low-KE electrons that are responsible for the main mechanism for cell death by causing DNA double-strand breaks. The model study of low-energy electron production was performed in experiments on water nanodroplets/ clusters of two different sizes – with 1000 and 3000 molecules/cluster- created using an adiabatic-expansion-based cluster source producing a jet of such particles. Following the ionization of the clusters by the intersecting synchrotron radiation of the FlexPES beamline, branch B, photoelectron spectroscopy of the species in the jet was carried out. The valence levels were ionized with several different photon energies in the range from ≈40 to 200 eV, thus producing photoelectrons with different kinetic energies. For the same photon energies, the signal of secondary electrons in the range of kinetic energies from 0 to 15 eV was recorded. These two types signals- from the valence and from the secondary electrons, when quantified, allowed to make a judgement on the efficiency of the secondary electron production.

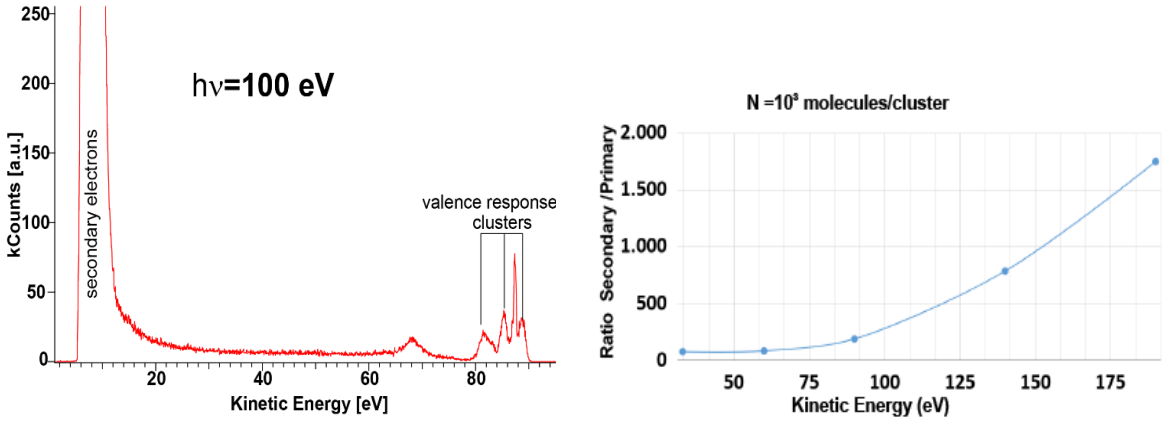

***Figure 4.4**: Left panel- an illustration of the spectra recorded in the valence and secondary-electron regions at h ν≈100 eV. Right panel – the ratio of the secondary to primary (valence) electron intensity for clusters with N≈10³ molecules/cluster at different kinetic energies of the primary valence electrons.*

The in-house research is performed by the beamline staff either with or without collaboration with the external user groups. Each staff member can get a (rather small) share of the overall 25% of the beamtime devoted to the maintenance, tests, developments and in-house research according to the general MAX IV policy. Several ongoing purely in-house research projects driven by the FlexPES scientists are listed below as examples:

Tb silicide nanowires on Si(110) (St. A.) The deposition and annealing of Tb on clean Si substrates leads to the self-organized formation of metallic Tb disilicide nanostructures. On planar Si(111) and Si(001), 2D films and two-domain nanowires form, respectively, so that vicinal substrates have to be used to grow single-domain nanowires. In contrast, the formation of unidirectional nanowires with

huge aspect ratios is possible using planar Si(110) substrates due to the reduced surface symmetry and the endotaxial growth of the Tb disilicide. These few-nm wide nanowires host quasi-1D electronic states. Thus, they are inherently unstable against, e.g., charge ordering (Peierls transition) at low temperatures. However, such 1D phase transitions compete with other magnetic transitions known for the Tb disilicide bulk phase.

Borophene on metal surfaces and at interfaces (A. P.) Borophene is a synthetic two-dimensional material composed of elemental boron arranged in a planar structure. In difference to graphene, it is particularly interesting for its polymorphism, which allows for the atomic-scale design of its structure and properties. It can be grown on a few metal substrates with quite different structural motifs, and the relation between structure and properties can be perfectly analysed by combining XPS, NEXAFS, ARPES and XPS. Two non-trivial systems (borophene on Ir(111) and honeycomb boron on Al(111)) were recently characterized at FlexPES[13], and now a new project with buried borophene films is emerging, as it has been discovered that borophene sandwiched between two metals (in this case Ir and Au) can nano-pattern the top metal film in a variety of ways, while the buried borophene retains its blanket-like 2D structure. This project greatly capitalizes on the possibility to grow and characterize samples in the MAX IV STM lab, and transfer well-defined samples for the spectroscopic characterization at FlexPES in a vacuum suitcase.

Au induced nanostructures on Si(110) (St. A.) The Au-Si(110) phase diagram for low Au coverages (≤ 1 ML) is known for 30 years, but the intriguing properties of the forming nanostructures is little explored. For about 1 ML Au, metallic nanowires grow and PES measurements revealed that they consist of Au silicide although there are no stable bulk Au silicides. Another metallic Au induced nanostructure is the 2x5 reconstruction observed for Au coverages slightly below 0.5 ML. This reconstruction hosts quasi-1D electronic states as found by ARPES. In between these two structures, the (4,0)x(±1,3) superstructure forms, which shows remarkable stability, e.g., against the adsorption of gases like O_2. Thus, it is a promising template for the ordered the growth of additional layers possibly enabling the nearly defect-free integration of organic semiconductors on Si. The (AR)PES studies at FlexPES are complemented by STM studies in the STM lab of MAX IV.

Zinc-nitride and zinc-oxide clusters for all-metal-oxide diodes and transistors (M. T., G. Ö.) Zinc nitride is a *p*-type semiconductor, for which there is a controversy around its gap: different sources report values from 1 to 3.2 eV. On the other hand, there is a significant interest in this material in connection to one of the latest "hot" semiconductor compounds—Zn oxide. ZnO is an *n*-type semiconductor, and in order to create a diode based on ZnO a possibility of *p*-type doping of it would be necessary, in which context nitrogen doping is of interest. Recently, a PES study of free Zn-nitride and Zinc-oxide clusters/nanoparticles, created in-situ by a dedicated setup attached to the ionisation chamber of the LDM-XPS setup, has been performed. The free (flying) particles have been studied by PES and then deposited and characterized again in a supported form. The optimal conditions for creating Zn-oxide and Zn-nitride clusters have been determined. Especially informative are the N 1s spectra of the deposited Zn-nitride particles, as Zn atoms could be observed in two different coordinations. Further investigations are ongoing to enable unambiguous assignment of all spectral features.

Angle-resolved photoemission from liquid samples (G. Ö., N. W.) The effect of solvation on the angular distribution of photoelectrons has not been extensively studied, and this in-house project aims to investigate this issue. We have recorded angle-resolved data for aqueous solutions of ammonium nitrate and a number of potassium salts of carboxylic acids (formic, acetic, propanoic, butyric, and

[13] A. B. Preobrajenski et al., ACS Nano 15, 15153 (2021).

hexanoic acid), using the liquid jet setup at FlexPES. In the first study, the N 1s angular distribution of ammonium nitrate was investigated as a function of photon energy, and for the two essentially bulk-solvated ions a slight difference in beta value can be observed, being slightly higher for ammonium than nitrate. This study is ready for submission and will hopefully be published before the end of the current year. The second study aims to compare the angular distribution of the bulk-solvated potassium ion with a progressively more surface-active carboxylate ion, from formate to hexanoate. The beta-formalism can strictly only be applied to a randomly oriented ensemble, which is clearly not the case for the surface-active ions, but the angle-resolved date will still yield insight into the process. The analysis of the data is in progress, and we aim to submit before the end of the year.

Self-assembly and On-surface Chemistry of Porphyrins (E. F) Porphyins are common molecules found in nature which perform key biological functions, such as within Haemoglobin and Chlorophylls. Porphyrins can be synthesized with a wide range of functionality, which, combined with their high thermal stability, makes them ideal for surface analysis. In this project porphyrin molecules functionalised with bromine atoms will be used to perform Ullmann coupling reactions and their underlying mechanisms. These processes will be studied initially by STM and then by XPS and NEXAFS at each stage of the reaction to gain a mixture of chemical and structural information. From this, details of the reaction mechanism will be studied. By observing these reactions on different surfaces the effect of the surface on the chemistry of these systems can be determined.

5 Points of concern

Before describing planned, proposed, or potential developments (as outlined in the next section), we present here areas where the beamline performance may not be optimal yet or where foreseeable risks for successful operation in the future can be identified. Although these points of concern are not critical for the present day-to-day operation, their understanding is essential for the proper prioritizing the development directions beyond the baseline expectations.

5.1 General: accessibility / throughput

The quality and the quantity of the accepted proposals define the overall scientific productivity of a beamline. While the quality can be increased by improving the performance of equipment and the level of user support, the amount of beamtime available for external users is pre-defined and can hardly be increased in the future. From the very first user call at FlexPES, we experience a considerable competition between user proposals, which keeps growing further, even with somewhat limited advertising from our side. As we are serving different user communities and proposals have to be submitted to different PACs, the beamtime must be shared in certain quotas between our two branches. For example, in the last call (Autumn 2022) we had 19 proposals from 16 different research groups submitted at the SMS branch but were able to schedule only 7. Although this situation is rather common for popular synchrotron beamlines around the world, it is hardly optimal for a new beamline trying to establish a thrilling research atmosphere and create its own strong community. Indeed, many users can get discouraged after a few unsuccessful applications and stop applying (especially first-time users), and our own outreach efforts remain limited deliberately. Another aspect of the too restricted access to the beamline is the lack of potential for developing new setups (as they will not increase the overall productivity). Therefore, certain solutions for increasing the user throughput shall be considered; they should be coordinated with other soft x-ray beamlines and should benefit MAX IV in general.

5.2 Beamline issues

5.2.1 Second-hand LPU

Within the scope of transferring and re-using equipment from the predecessor MAX-lab facility, FlexPES has inherited an LPU from one of its beamlines. This is a simple planar undulator delivering photons with linear horizontal polarization only. It got a new magnetic structure in 2010 and was refurbished and fully characterized before installing into the 1.5 GeV ring of MAX IV. Still, although the aging of mechanical components is not critical yet, it can already manifest itself in infrequent but dangerous unintentional tapering of the device. Being a viable and economic solution in the initial phase of FlexPES operation, this device cannot be considered satisfactory at the world's first fourth generation synchrotron facility on a long run, due to its lack of full polarization control and potential aging issues. The full control over the x-ray polarization is obviously necessary to enable all flavours of linear and circular dichroism in x-ray absorption and photoemission for systems possessing structural or magnetic order, thus broadening the toolbox of the user community, and stimulating creativity in the design of user experiments.

5.2.2 Lack of flux at higher energies

As only one (re-used) diffraction grating was covering the entire photon energy range in the initial phase of operation, we had to compromise at both low and high ends of the spectral range. With the new 400 l/mm grating installed in the summer 2022, we hope to largely increase the flux below 200 eV. With the low-energy flank secured, it would be natural to shift the main working range of the 1200 l/mm grating to somewhat higher photon energies to enable more flux above 1000 eV. An enhanced flux at the high-energy end is desirable primarily for the XPS studies on low-density targets like liquid and molecular jets, and for the NEXAFS studies with the fluorescent-yield (Si drift) detector. A new 1200 l/mm grating with a smaller blaze angle and improved reflectivity could make the overall intensity distribution of the beamline flux more homogeneous and be a better match to the 400 l/mm grating.

5.2.3 Heat-load deformation of M1

The horizontally deflecting mirror M1 is taking large heat load and its temperature can reach as high as 40 °C at low photon energies with the typically used acceptance (and even higher at full acceptance). This may result in the M1 pitch drifting away from the nominal position leading to intensity loss. It is especially challenging to work with frequently alternating low and high excitation energies. An ideal solution would be a design improvement of the M1 holder and the cooling system. A promising mechanical modification of the M1 chamber components was suggested at the Veritas beamline, and we are looking into a similar development. Less straightforward but easier to implement is to continuously adjust the M1 pitch by using a feedback signal from two horizontal beam monitors positioned downstream symmetrically to the beam.

5.2.4 Gas-sending systems

Gas delivery is a critical part of experimenting on both SMS and LDM branches. At MAX IV, the construction of gas-delivery systems at individual beamlines (fire-proof cabinets, gas lines, mixing and dosing equipment, pressure gauges, etc) is delegated to a large extent to the laboratory level, in order to ensure common standards in parts, quality and safety. Unfortunately, this delegation resulted in numerous delays in the past, and the originally foreseen systems are still not in place in full scope. As a temporary solution we had to build small ventilated cabinets for mini gas cylinders and to implement a rather primitive (manual) handling of gases. Although it may be sufficient to large extent for the SMS branch, the LDM branch end stations usually consume large amounts of gases in their experiments and do need proper gas delivery systems. At present, using large cylinders with even relatively harmless gases always requires considerable re-connection efforts and associated considerable

paperwork to follow safety regulations. Whenever it comes to more dangerous gases, the amount of work and bureaucracy is escalating drastically, and users often refrain from submitting non-standard proposals for this reason.

5.3 End station issues

5.3.1 EA01: main manipulator problems

The main manipulator is rather old and has some issues. For small or inhomogeneous samples the main problem is a lack of precision and reproducibility resulting from the incremental encoders on the motors. We can hardly guarantee reproducibility within 50 um, and with the focussed beam on the order of 50 x 20 um this is challenging for finding interesting spots on the sample. There is a clear need in improving the manipulator performance, and this can be done by equipping it with some absolute encoders. Another issue is a gradual loosening of fixation of the sample plates on the manipulator head upon frequent sample exchange, which can result in undesirable sample movement and even loss of the thermocouple read-out in the middle of experiment. Here a re-design of the sample head is probably needed to increase the rigidity.

It should also be noted that as a four-axis manipulator, it is not optimized for ARPES studies but rather for easy and fail-free sample transfer (i.e., higher throughput) and wider temperature range in more standard PES and XAS experiments. On the other hand, with more flux at low energies (due to the new 400 l/mm grating), better heat-load stability (due to planned improvement of the M1 chamber design) and the modern DA30 electron analyser, the attractiveness of doing ARPES in this station may grow. In this case, a construction of a second manipulator enabling azimuthal sample rotation may be considered.

5.3.2 EA01 and EB02: Analyser software deficiencies

The spectrometers on the EA01 and EB02 end stations are currently controlled by the native SES software by ScientaOmicron. It has a number of severe limitations/shortages:

- Complex automated measurement sequences involving changes in several beamline/end station parameters are not possible. Users often are forced to manually perform tedious data collection in cases where it could and should be completely automated.

- Complex experiment's parameters change such as fast raster scanning, moving sample or some other beamline element on a nonlinear trajectory is not possible.

- Lack of stability (crashes) and lack of interlock options (like protecting detector from overexposing).

- File formats and metadata: Only a few pre-defined data file formats, with only a small subset of the beamline configuration included in the metadata. A support of a wider range of formats such as NeXus to allow recording all relevant metadata is necessary.

5.3.3 EB02: old analyser as a limiting factor for the LDM research

The core of the EB02 end station was built at the old Max-lab more than 25 years ago, and has since then been extensively used by scientists in the fields the atomic/molecular physics, liquid surfaces, free nanoparticles, and materials science. 400+ publications have been published on the results obtained at this end station. In the process of relocation to MAX IV, the end station was attached to

the B branch of the FlexPES beamline, in order to enable access to the new facility for LDM researchers without much delay. However, in recent years the research interests of many user groups have shifted towards experiments with target concentration reaching (and exceeding) the limit for our UHV PE spectrometer (R4000) with the available pumping capacity. Due to the limited resources upon the relocation, the main parts of the end station (the UHV electron spectrometer and the analysis chamber) could not be upgraded at that time. At MAX-IV, the limitations of the old spectrometer and design became especially obvious with the increased number of groups with the liquid-jet experiments, and with the materials-science users turning to beamlines with NAP (Near-Ambient-Pressure) spectrometers. Realizing the demands, in September 2021 an initiative group organized a workshop to discuss the endstation upgrade. More than 30 participants took part in the workshop from several Swedish and foreign universities outlining their visions for the upgrade. The workshop made it clear that a new analysis chamber with a NAP spectrometer would qualitatively increase the possibilities in a wide spectrum of activities and attract a substantial number of new proposals.

6 Developments: ongoing, planned and possible

In this section we describe beamline developments of different kind. Some of them are already in the planning and got funding, while the others are less certain and need a fair evaluation and prioritization. This is where we would be especially grateful for an input from the Review Panel. The majority of planned or suggested upgrades stem from the known deficiencies listed in the previous section.

6.1 Missing baseline capabilities

Despite two years of general user operation, there are a few things promised but not fully delivered to the users in the baseline configuration. Fixing these shortages is obviously the high-priority projects, which go before any really new developments.

6.1.1 Completing the gas-sending systems

To overcome the shortages in the gas delivery systems described in the “Points of Concern” section, a dedicated project has been started at FlexPES in August 2022. Its scope includes the following developments:

- Two primary gas cabinets with four gas lines each: drawings, risk assessment, 3D modelling, purchase, component installation, PLC integration, testing.
- Upgrade of the existing gas panels at the SMS branch: adding pressure transmitters with readout and extra connections to enable using gases at the open port (EA02 station) in the future.
- Two new gas panels at the LDM branch enabling gas mixing, with pressures up to 10 bar: drawings, risk assessment, 3D modelling, purchase, component installation, testing.

This project will benefit specifically the gas-phase experiments at the LDM branch, enabling gas mixing and higher gas pressures. It should also ensure extra safety in the gas handling. The project is fully funded at the laboratory level and expected to be finished by the summer 2023.

6.1.2 Stabilizing photon flux intensity

As mentioned earlier, a lack in the photon flux stability is to be traced back to the overheating of the M1 mirror mechanism, resulting in a gradual variation of the M1 pitch with time. There is a proposal of improving the M1 chamber design, which is now under discussion with the chamber manufacturer (FMB). In the original design, the electron-collecting screen in front of the mirror is rigidly connected

to the mirror holder. At high incident intensities, it gets overheated, somewhat deformed, and translates this deformation to the mirror holder. In the preliminary new design the screen is detached completely from the M1 mechanism and equipped with a dedicated water cooling loop (while still electrically insulated). It is expected that this modification of the M1 chamber components should reduce the maximum temperature on the screen from over 100 °C today to some 35 °C, and the heat-induced stability issues can be completely eliminated. Obviously, this will drastically improve spectral quality and enable extracting quantitative information more reliably. The costs for this project are on the scale of 20 kEuro, but the funding is not secured yet. With some luck, the project can be realized already in the beginning of 2023, otherwise in the next summer shutdown.

6.2 Short-term and middle-term developments

Here we describe possible upgrades to either the beamline or the end stations, which can be realized on the horizon of 1 to 3 years, and which can provide a considerable gain in the FlexPES capabilities at reasonably moderate costs.

6.2.1 New grating for high-E range

As described in the previous section, the old 1221 l/mm grating can be replaced with a new one. Higher manufacturing quality in combination with a smaller blaze angle would enable better reflectivity and a certain shift of the high-flux range to somewhat higher energies. As the low-energy part of the beamline spectrum is now secured by the new 400 l/mm grating, such a replacement is meaningful and can give a gain by factor 2 at around 1000 eV. This would benefit XPS studies at both branches, but specifically the research on diluted targets.

6.2.2 In-house developed PE analyser software

In order to overcome shortages (see “Points of concern”) of the proprietary SES software used on two of our analysers, we have an ongoing project aimed at developing a comprehensive control software in-house. The natural solution here is based on the use of new PEAK software from ScientaOmicron. Due to its network-based architecture it may be rather straightforward to integrate it into the beamline’s Tango control system, thus enabling full control over all beamline and spectrometer parameters within the same software layer. A general MAX IV project on integration of hemispherical analysers’ software in the Tango control system on several beamlines has already been started. This project includes two main developments: the spectrometer’s Tango device server part (using PEAK as an intermediate layer), and a graphical user interface, which would support more diverse and fully automated photoemission experiments. The FlexPES staff is deeply involved in this development; the project has to be delivered to users in 2023.

6.2.3 Added positioning precision in EA01

A great improvement in the sample positioning precision and motion reproducibility of the main manipulator in EA01 is necessary, and can be achieved by upgrading the existing incremental encoders on all axes with suitable absolute encoders and scales. As we prefer to keep the possibility of joystick operation (in addition to the standard computer control), we would like not to use the standard MAX IV motor controllers, but rather upgrade our present units with the cards capable to read absolute encoder position values. We are working now on a prototype for one axis, and expect the solution to be in reach very soon. Once realized, this upgrade must eliminate any unintentional variation in the sample positioning, which is very important for small or inhomogeneous samples. The expenses are on the scale of 10 kEuro; we have applied for this upgrade in the FlexPES operation budget 2023.

6.2.4 Thermo-programmable desorption capabilities

One popular type of experiments in the EA01 end station is T-dependent mapping of on-surface reactions with XPS. While this method can reveal chemical transformations in the species on the substrate surface, the desorbed species cannot be detected simultaneously. To reveal the complete picture of reactions, it would be highly desirable to complement these experiments with a simultaneous detection of the desorbed species with mass spectroscopy (doing XPS and TPD simultaneously). This would be a unique setup at MAX IV, as no other beamlines offer a combination of T-dependent XPS with TPD. The newly upgraded main vacuum chamber of the end station is already foreseen with a port for TPD studies, and the only missing equipment is a suitable mass spectrometer. It has to be retractable, highly sensitive to small amounts of desorbed species, effectively shielding parasitic signals from the surrounding, and reasonably fast. Therefore, a simple RGA analyzer is not optimal for this purpose, and a rather sophisticated mass spec dedicated for UHV-TPD studies is necessary for the best possible experimental outcome.

As for now, some 3 to 4 user groups will readily be using TPD as a compliment to the T-dependent XPS. Importantly, the TPD mass spec will be used in parallel with the XPS measurements, therefore no beamtime will be lost. On the other hand, adding TPD as an additional channel of information about studied systems may be attractive and rather unique feature. If we manage to get good results, we also can promote this feature in the community advertising for more and better user proposals. On the whole, it would strengthen the position of FlexPES as an “all-in-one” spectroscopy beamline and has a potential to broaden the user community, specifically with groups focussed on catalytic on-surface reactions. The estimated project budget is 30 kEuro; we applied for it in a dedicated (“beamline upkeep”) process, and decision is expected towards the end of 2022.

6.2.5 Near-ambient pressure NEXAFS prototype setup

The open port (station EA02) at the SMS branch is not in use for now, but has a potential to house an additional experimental setup. It is probably inappropriate (at least for now) to construct here an expensive and highly-demanding end station, because with the same amount of the beamtime available at the SMS branch it may increase the scientific productivity only marginally and won’t justify the effort. Much more relevant would be a simple setup with added functionality, which can be efficiently used by the groups already working on the upstream station (EA01). Also important is that this setup shall not increase the workload on the staff significantly (i.e., be simple in operation).

Therefore, we consider constructing at the open port a prototype setup for high-throughput NEXAFS measurements including experiments at non-UHV conditions and even up to the near-ambient pressure (NAP). The experimental chamber will be separated from the beamline by a thin silicon nitride membrane, which can withstand atmospheric pressure (we already tested that it works for some commercially available 100 nm thick membranes). The detectors will be total- and partial-electron yield (the latter for vacuum measurements only) and an energy-dispersive fluorescent detector. With the fast scanning NEXAFS capabilities developed at FlexPES for a variety of detectors, this station will ideally fit the beamline profile and assist users in two main cases:

- Simple in-vacuum NEXAFS measurements with high throughput. As the main experiment is running in the upstream station EA01, a set of (e.g. reference) samples can be loaded at EA02, and whenever there is a pause in the main measurements, the NEXAFS spectra from these samples can be recorded. The process can be further automated for higher throughput. This will enable more efficient usage of the beam time, which otherwise is inevitably lost on the sample transferring and positioning. Another advantage of this approach is that non-UHV compatible samples can be measured without any risk of contaminating the UHV chambers.

Finally, some extra samples from other users can be measured (e.g. for feasibility studies) without interfering with the ongoing main project.

- Pressure-dependent and temperature-dependent variations in the NEXAFS spectra can be followed, with the pressures at least up to several mbar. This is a more demanding mode of operation, but it will add a new angle to the studies of real-life materials for catalysis, batteries, solar cells and sensor applications.

The NAP-NEXAFS setup would not require much resources. Primarily – CAD design, and then some hardware: simple analysis and introduction chambers, a support with positioning for the SiN membrane relative to the beam, a manipulator, some pumping, gas delivery equipment, etc. Luckily, it can be designed and built gradually (in a modular fashion) and without stopping the normal user operation. The core of the system can be built for around 100 kEuro within a year.

6.2.6 Liquid jet setup

Liquid jet photoelectron experiments have been performed at MAX IV and before that at MAX-lab since 2006 and have yielded substantial scientific output in a variety of fields. However, there are limitations with the current experimental setup that we are currently trying to overcome:

The jet we have so far used is cylindrical in cross section, which means that the take-off angle of the electrons from the surface in the direction of the spectrometer vary from grazing to normal, since the whole width of the jet is illuminated (x-ray spot much larger than jet diameter). The probing depth varies with the take-off angle, meaning the measurement will be an average of all situations and less sensitive to variations in surface concentration.

After injection into vacuum, the liquid sample is collected in a liquid nitrogen cooled trap, which has a limited capacity. With the liquid flow we normally use (0.5-0.6 ml/min) it fills up in ≈12-15 h, after which we must break vacuum to replace it.

Flat-jet development

To obtain a more well-defined geometry for our photoemission experiment, we are developing our setup to operate with flat jets, and we are pursuing a couple of different avenues to achieve this. A sufficiently thin flat jet (≤1 μm) could allow soft x-ray absorption measurements in transmission, and this is also part of the scope of this project. A proposal to Carl Trygger's Foundation was granted (ca. 60 kEuro, CTS 20-502), giving us financial means to go ahead with this development project. We have tested commercial flat-jet nozzles from Micronit GmbH in June this year and have been able to show proof-of-principle operation (see Figure 6.1). Unfortunately, these nozzles have the drawback of requiring a high flow to produce a sufficiently large sheet with stability, which increases the vapour load on the system. In practice, aqueous solutions are just barely possible to run with acceptable vacuum for the spectrometer, and samples with higher vapour pressure would be even more difficult. The larger sample consumption also means that the cold trap fills up faster, reducing the measurement time before having to exchange the cold trap.

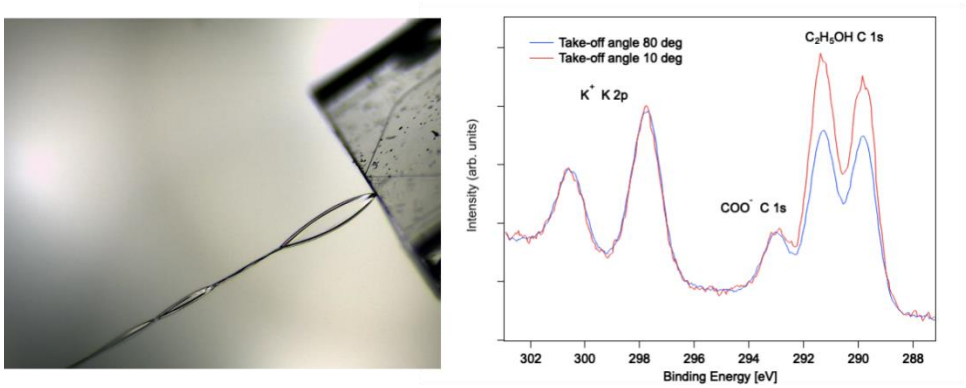

***Figure 6.1**: Left: Sheet produced by Micronit nozzle (photo from Micronit GmbH). Length of first sheet is ≈0.5 mm, width <0.2 mm. Right: Spectra for 0.4 M KCOO in a 0.2 mol % solution of ethanol in water recorded with near-normal and grazing take-off angles at FlexPES in June 2022, normalized on the K 2p features. At low take-off angles, the surface-active ethanol molecules become more prominent compared to the K+ and COO- ions, which avoid the surface.*

We have also started a collaboration project with the Sample Environment and Characterization group at XFEL to modify the Gas Dynamic Virtual Nozzles (GDVN:s) they have developed (for sample delivery in e.g. protein crystallography) for use in soft x-ray spectroscopy applications. The nozzles are 3D-printed at XFEL and can be customized relatively easily. The LU PhD student Tamires Gallo (supervisors G. Öhrwall and N. Walsh) has taken part in testing and characterization of the new nozzles, which were designed taking the characteristics of the FlexPES system into account (see Figure 6.2). These new nozzles require a substantially lower flow rate than the Micronit nozzles, also lower than the cylindrical nozzles we use today (0.2-0.3 ml/ min compared to 0.5-0.6 ml/min). They have been tested with several solvents and operate stably under vacuum, and we will perform the first tests at FlexPES during autumn 2022, hopefully being able to offer them to users already in spring 2023.

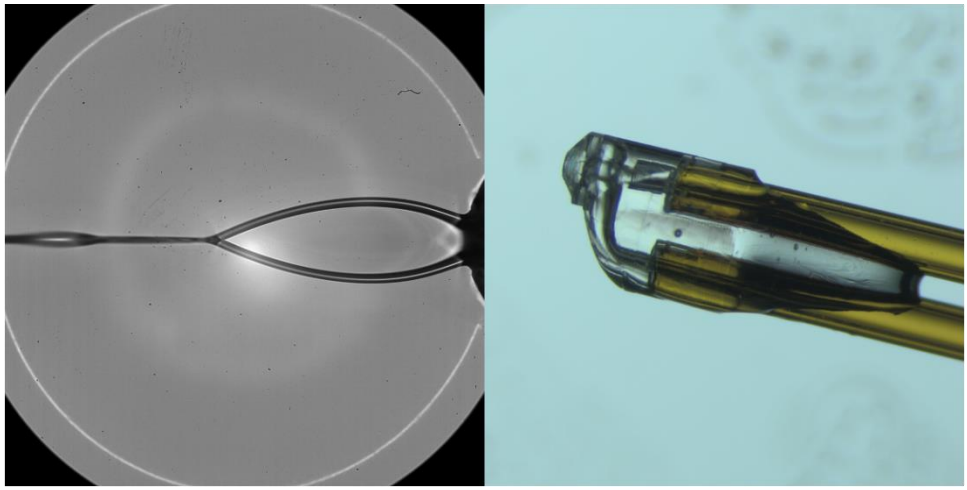

***Figure 6.2**: Left: Sheet produced with the new XFEL GDVN. The length of the sheets is approximately 0.5 mm and the width 0.2 mm. Right: Microscope picture of the nozzle. The width of the nozzle body is ≈1.2 mm, the connecting tubes (yellow) have a diameter of 360 µm.*

Liquid catcher development

To address the issue with the cold trap, we are designing a "catcher", a receptacle that will catch and extract the liquid from vacuum, and deposit it into a vessel outside. Such systems are available commercially but are quite expensive, and would have to be extensively adapted due to the size constraints at the FlexPES. The design follows existing systems closely, with the catching part sitting

on an in-vacuum XYZ translation stage, as shown in Figure 6.3 below. The system is intended to work both with the cylindrical jet nozzles and the flat jet nozzles. The CAD design is in progress, and we hope to test the system in spring 2023.

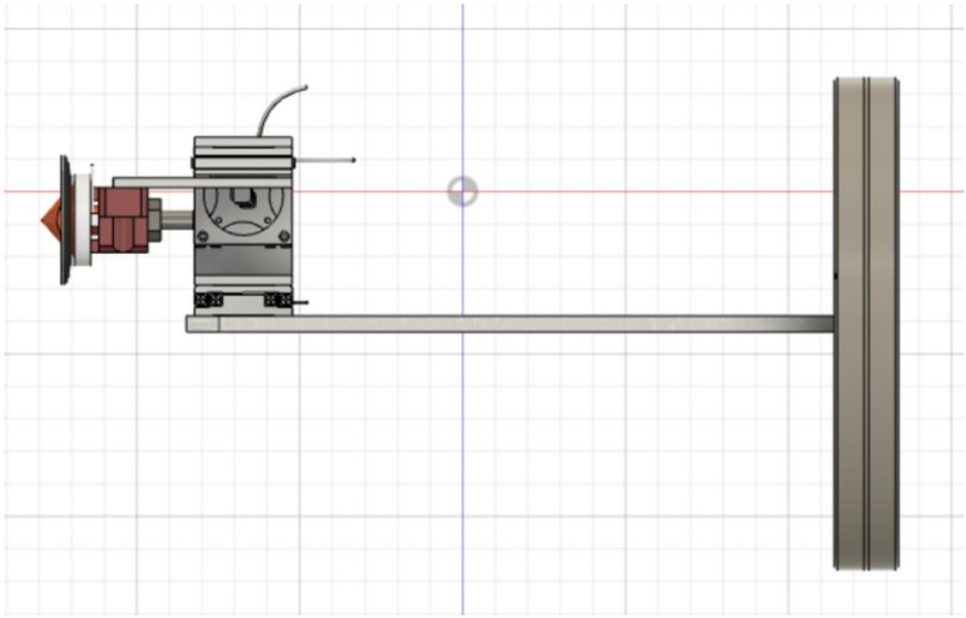

***Figure 6.3**: CAD sketch of the liquid jet catcher. The catching unit is mounted on translation stages from Attocube Systems AG, and is heated to a suitable working temperature with a ceramic heater from Bach Resistor Ceramic GmbH. It will be mounted on a DN160CF flange with electric and liquid feedthroughs (not included in sketch) to fit at the FlexPES B-branch photoemission end station.*

6.2.7 NAP spectrometer replacing Scienta R4000 at EB02

As mentioned above, after the EB02 transfer from the old lab, the main emphasis was first on providing the so-called "gas-phase" users with the possibility to resume their activities. These included the studies on molecular/cluster, liquid, and nanoparticles jets, as well as on the separate molecules using a gas-cell. Later, the EB02 end-station was upgraded and refurbished responding the demands to its earlier users from another field- of supported samples – prototypes for novel batteries, solar cells, and organic electronics.

While the variety of research performed at EB02 is large, two types of it have been constituting its long-standing and peculiar part – the studies using the liquid-jet setup and the studies of free nanoparticles in a beam. In the liquid-jet experiments, phenomena such as enrichment and alignment at the liquid surface are studied. The most common solvent used in the liquid-jet studies has been water, demanding a complicated differential pumping arrangement to be installed in the endstation to maintain sufficiently low pressure inside the electron spectrometer. The use of the other solvents with the higher vapor pressure than water is practically impossible. Replacement of the current Scienta R4000 UHV spectrometer by a NAP spectrometer would allow to broaden the range of solvents and significantly simplify the installation and operation. Also, the free-nanoparticle project has developed over time, with multicomponent particles out of alloys and metal compounds being studied. The nanoparticle production is based on vapor aggregation in a gas mixture, which creates a high gas load at the limit for the current spectrometer, and its replacement by a NAP instrument would principally broaden the range of substances to be studied at nanoscale, in the absence of the support influence. The estimated cost for a new spectrometer is about 350 kEuro.

6.2.8 ICE end station developments

- A future aim (with a target date of 2024) is to offer a more specialized access to the ICE spectrometer that will involve tailoring the setup for user experiments. Such an approach would involve pre-simulations using the SIMION software package in order to determine the most suitable electric field configuration, subsequent adaption of the setup and testing. This will be a time-consuming activity and therefore, extra manpower is necessary to make this possible.
- Installation of larger MCP's. The ICE setup currently uses MCP's of 75 mm in diameter. Increasing the diameter of the MCP's to 100 mm would enable the detection of higher energy particles (using the same electric and magnetic field conditions as used today). The cost of replacing the current MCP's with larger ones is ~30 kEuro.
- Upgrading ICE to a high-voltage spectrometer for the detection of higher energy particles (100's of eV). Expected cost 30-40 kEuro (for new detector arrangements, feedthroughs, power supplies etc).

6.2.9 TRISS – TRapped Ion Spectrometer Setup

In 2021 the Swedish Research Council awarded ca. 1 MEuro to the TRISS project. The TRISS project is currently underway and will deliver a mobile suite of instruments that enable trapped ion research at MAX IV. The experimental setup will comprise an electrospray ionisation source, ion optics, a segmented ion trap and a Reflectron Time of Flight spectrometer (ReToF). The setup is foreseen for experiments at both FlexPES and Veritas beamlines and will be used to study various systems that are not accessible by other means, for example molecular ions, biomolecules, nanoscale clusters and radicals.

6.3 Major development possibilities

The following major developments require considerable funding and can be realized in a longer perspective (exceeding three years).

6.3.1 Elliptically polarizing undulator as a new x-ray source

The lack of full polarization control and potential aging issues of the present x-ray source mentioned in the "Points of concern" call for a replacement of this device with a reliable modern undulator enabling different light polarization. We consider an elliptically polarizing undulator (EPU) of the APPLE II type, similar to the insertion devices used at other four beamlines on the 1.5 GeV ring. An access to various polarization modes will enable all kinds of linear and circular x-ray dichroism experiments, and provide much better options for ARPES and ResPES, thus broadening the toolbox of the methods at FlexPES considerably. According to our estimates, some 30% of the user proposals will benefit from the new capabilities from the very beginning, and on the long run the availability of an EPU will stimulate designing more sophisticated and elegant experiments by the proposers.

The magnetic period of the EPU is balancing the lowest accessible energies versus the photon flux at higher energies. As FlexPES optics is designed for energies above 40 eV, and because there are already beamlines optimized for low energies at MAX IV (FinEstBEAMs and Bloch), we consider the optimal period of the EPU to be ~54 mm. This should enable horizontal polarization from ~40 eV, vertical – from ~70 eV and circular – from ~55 eV, as a compromise between the access to relatively low energies (e.g. for ARPES) and sufficiently high flux at higher energies.

An initiative for a new EPU was submitted as a so-called "Expression of Interest" (EoI) to be included on the MAX IV roadmap for the years to come. It was evaluated along with other EoI and graded

relatively high, but it is still not decided yet whether and how the new x-ray source for FlexPES shall be placed on the MAX IV roadmap. In this sense the opinion of the Review Panel on the importance of this upgrade may represent an important input for the decision makers.

6.3.2 New end station at EB02

As discussed above, a replacement of the present Scienta R4000 spectrometer with a NAP spectrometer would widely expand the range of possibilities at EB02, without any additional changes to the end station. A further qualitative step in removing limitations and expanding the variety of experiments with the liquid jet, as well as the cluster and nanoparticle beams, could be achieved by replacing the whole end station, including analysis-, preparation, and introduction chambers, with the new NAP spectrometer as the main instrument. Moreover, new experiments with the supported samples in gaseous environment or outgassing would become possible. The new analysis chamber should possess larger ports than the current end station (CF200/250 against CF100/CF150) and more open geometry, allowing mounting of different sample introduction systems and providing sufficiently large permanent pumping capacity. It should also allow ease of movement for alignment purposes, and flexibility in orientation with respect to the photon beam, for e.g. studies of angular distributions, including non-dipole effects. Such an upgrade of the end-station was discussed at a workshop organized by FlexPES users in September 2021, and an Expression of Interest proposal within the framework of the Strategic development program at MAX-IV was submitted to the Lab management in November 2021. This upgrade would clearly demand a considerable investment, substantially more than just the exchange of the spectrometer.

The aim of the upgrade of the EB02 (B-branch) end station is not only in the improvement of the capabilities for the currently regular types of experiments, but also in attracting a new category of users to the FlexPES B-branch, who today would rather apply for beam time at conventional APXPS beamlines. At the new EB02, the tools for sample manipulation and treatment would be less specialized and sophisticated than those offered at the other APXPS end stations, but would instead be amenable for exploratory work where user-provided ancillary equipment, e.g. for uncommon sample preparation, could be hosted with relative ease. For the current users of the end station, the upgrade would extend the range of possibilities in terms of, e.g., using more volatile solvents in the liquid jet measurements or obtaining higher pressures to produce certain clusters/nanoparticles studied in a beam. It would also simplify and make more efficient many of the experimental procedures, saving precious beam time used otherwise for repeating mounting and dismounting ancillary equipment.

6.3.3 New dedicated LDM beamline

Since FlexPES opened to general users in Spring 2020, the total number of beamtime proposals using AMO/LDM[14] equipment has steadily increased. With the ICE end station now also available to general users (FT22), the number of proposals for AMO/LDM research increased once more - 12 proposals for LDM experiments at FlexPES B (4 x liquid jet XPS, 4 x free nanoparticle XPS and 4 x ICE end station). In addition, the FlexPES B branch also caters to XPS experiments on surfaces and thin films, and in the same call, 4 proposals were submitted for such research (i.e. a total of 16 proposals were submitted to FlexPES B compared to 19 proposals for FlexPES A). With only 12 weeks of beamtime available on FlexPES in FT22, this means that of the 12 LDM proposals submitted, only 3 were awarded beamtime (1 x liquid jet and 2 x ICE) – a meagre outcome despite so much interest from our research community. Indeed the FlexPES A branch also suffers from this co-existence - only 7 of their 19 submitted proposals

[14] AMO/LDM: gas phase molecular/cluster/nanoparticle/ liquid jet/ aerosol measurements

were awarded beamtime. At FinEstBeAMS (– another double branched, multi-endstation beamline) - the situation is similar. LDM research (using GPES) competes with both photoluminescence (PLES) and surface science (SSES) research. Moreover, as the currently available equipment produces more research output, this upward trend in submitted beamtime proposals is likely to continue.

In addition to the equipment that is currently available to general users, the LDM team have a number of ongoing development projects that will offer new capabilities to our user community. Within the next 6-26 months a variety of new setups will be available to general users including an aerosol sample delivery system[15] (expert commissioning Spring 23), the liquid flat jet setup and TRISS - the VR-funded mobile ion trap end station[16]. These new pieces of equipment are already attracting significant attention from our user community: we expect to receive at least 3-4 expert commissioning proposals for the aerosol sample delivery system; the user community have already engaged in proof-of-principle tests using a flat jet test setup at FlexPES B; and a number of existing, as well as new users have proposed interesting science cases for the ion trap setup.

Unsurprisingly, we anticipate that as our LDM equipment repertoire expands, so too will the demand from our user community for access to beam time. However, since AMO/LDM equipment is somewhat parasitic on different beamlines and competes for access with a number of other research fields, we recognise that a critical point is imminent/is already reached, where we will fall far short of catering to the needs of our expanding LDM community and we will not be able to facilitate a strong research output. For this reason, we recognise that if we are to adequately cater to the needs of our user community and simultaneously nurture the development of AMO/LDM research at MAX IV, it would make sense to build a dedicated beamline that caters specifically to our evolving LDM research community.

6.4 Prioritization of the development projects

A summary of the ongoing, planned and possible development projects is given in Table 5. In the "Active" category we put the funded ongoing projects, to illustrate the present development activities at FlexPES. All other projects are not funded yet, and therefore need a thorough prioritization. The short- and middle-term projects are grouped into four categories according to their priorities, as it is seen by the BL team. Highest ranked are the projects, which expect to benefit many user groups at a moderate cost and labour. The last group are the more expensive, more long-term, but also potentially more beneficial projects, something that can become a game-changer in the more distant future. We are specifically interested in the opinion of the Review Panel on the i) suggested priorities for the moderate-cost projects and ii) the potential of the large-scale developments to make a big and positive change to the way we operate today.

Table 5: Overview of ongoing and planned development projects at FlexPES

Project	End station / beamline	Required funding and resources	Status
Active			
Gas handling systems	All end stations	Central Project Office (CPO) coordinated; resources secured	In progress
PE analyser software integration	EA01, EB02	CPO coordinated; resources secured	In progress

[15] Part funded by Crafoordska Stiftelsen (20210617) and developed in collaboration with Ergonomics and Aerosol Technology, LTH.
[16] TRISS, VR 2021-00277

TRISS – Trapped Ion Spectrometer Setup	Mobile end station	Externally funded, resources secured	In progress
Flat liquid jet setup	EB02	Externally funded, resources secured	In progress
Added positioning precision	EA01	Approved (?) in the budget 2023, need KITS resources	Ready to go
Highest priority			
M1 T-stabilization (M1 chamber re-design)	Beamline	15 kEuro, minor need for common resources	Awaiting MAX IV decision in 2022
Justification: all users will gain from the flux stability, as there will be no need to adjust the optics for different LPU gaps, design is ready, the work can be realized already in the winter shutdown			
High priority			
NAP spectrometer for high gas loads	EB02	Ca. 350 kEuro, minor need for common resources	Plans to submit a grant application
Prototype NAP-NEXAFS setup	EA02 (new, on the open port)	Stage 1: CAD design resources Stage 2: ca. 100 kEuro (proof of principle)	In consideration
Justification: both projects represent rather ambitious further developments with the potential to broaden experimental capabilities considerably; they are known to be feasible, and are considered to be of strategic importance for securing attractiveness of the BL in the next 5-10 years.			
Medium priority			
Thermo-programmable desorption capabilities	EA01	Ca. 40 kEuro; minor KITS and PLC resources	Awaiting MAX IV decision in 2022 (“upkeep”)
Justification: can be done quickly and at relatively low cost; several surface-science groups will be gaining extra information along with T-dependent XPS			
High-voltage TOF spectrometer (upgrade)	EB01 (ICE)	Ca. 40 kEuro	In consideration
Justification: would broaden the ICE-related user community visibly			
Lower priority			
New 1200 l/mm grating	Beamline	Ca. 70 kEuro	In consideration
Justification: May increase the flux by a factor 1.5-2; would be beneficial for all users. The lead time > 1 year			
New (larger) MCP detectors for the TOF spectrometer	EB01 (ICE)	Ca. 30 kEuro	In consideration
Justification: would broaden the ICE-related user community visibly			
Large-scale projects			
New x-ray source (EPU)	Beamline	Ca. 1 MEuro	In consideration
Justification: would solve aging issues of the present ID, provide full polarization control, higher scanning speed. Would benefit all users, but specifically (polarization control) – some 30% of users. Would contribute to attracting new users. Can be realized on the scale of 3 years once funding is secured.			
New end station around the NAP spectrometer	EB02	Ca. 0.8-1 MEuro	In consideration
Justification: Would extend the range of possible experiments and simplify many of the experimental procedures, saving precious beam time. The gained flexibility would attract new categories of users to the FlexPES B-branch, something they cannot find today at standard AP-XPS setups.			
New LDM beamline	MAX IV	Ca. 8 MEuro	In consideration
Justification: Would increase access to synchrotron light for all end-stations and spectrometers discussed in this joint review of FlexPES and FinEstBeAMS, thereby facilitating the growth of the associated communities. The current and planned ‘mobile’ end stations would have a more permanent home on a specific beamline. A dedicated beamline would be optimised to provide optimal conditions for gas-phase and liquid jet measurements.			